Translation of focused ultrasound for blood-brain barrier opening in glioma

Caterina Brighi

ACRF Image X Institute, Sydney School of Health Sciences, Faculty of Medicine and Health, The University of Sydney, Sydney, NSW 2050, Australia

Ekaterina Salimova and Michaelde Veer

Monash Biomedical Imaging, Monash University, Clayton, VIC 3800, Australia

Simon Puttick

CSIRO Probing Biosystems Future Science Platform, Herston, QLD 4029, Australia

Gary Egan

Monash Biomedical Imaging, Monash University, Clayton, VIC 3800, Australia and School of Psychology, Monash University, Clayton, VIC 3800, Australia

Keywords

Preclinical focused ultrasound; Blood-brain barrier; Glioblastoma; Drug delivery; Immunotherapy; Sterile inflammation

Abbreviations

Ab antibody; AEC acoustic emission controller; AP acoustic pressure; BBB blood brain barrier; BBBD blood brain barrier disruption; BL burst length; CE MRI contrast enhanced magnetic resonance imaging; DCE-MRI dynamic contrast enhanced magnetic resonance imaging; EB Evans blue; FUS focussed ultrasound; GBM glioblastoma multiforme; Gd-DPTA gadopentetate dimeglumine; GEMMs genetically engineered mouse models; GNP gold nanoparticles; IHC immunohistochemistry; IHM in house manufactured; IP intraperitoneal; IV intravenous; MB microbubbles; MI mechanical index; MT magnetic targeting; MRIgFUS MRI-guided focused ultrasound; PNP peak negative pressure; RF resonant frequency; PCS passive cavitation detection; PET positron emission tomography; PFS progression free survival; PRF pulse repetition frequency; SES single-element spherical; SIR sterile inflammatory response; SPIO superparamagnetic iron oxide; T total sonication time; T2W-MRI T2-weighted MRI; TB Trypan blue.

Highlights

• More clinically relevant models of glioma are needed for preclinical FUS studies.

• Methods standardization for FUS delivery is required for clinical translation.

• Preclinical FUS evaluations should use clinically translatable in vivo imaging methods.

• FUS can induce a beneficial anti-tumour immune response in glioblastoma.

• FUS can be used to allow delivery of targeted immunotherapies in glioblastoma.

Abstract

Survival outcomes for patients with glioblastoma multiforme (GBM) have remained poor for the past 15 years, reflecting a clear challenge in the development of more effective treatment strategies. The efficacy of systemic therapies for GBM is greatly limited by the presence of the blood-brain barrier (BBB), which prevents drug penetration and accumulation in regions of infiltrative tumour, as represented in a consistent portion of GBM lesions. Focused ultrasound (FUS) – a technique that uses low-frequency ultrasound waves to induce targeted temporary disruption of the BBB – promises to improve survival outcomes by enhancing drug delivery and accumulation to infiltrating tumour regions. In this review we discuss the current state of preclinical investigations using FUS to enhance delivery of systemic therapies to intracranial neoplasms. We highlight critical methodological inconsistencies that are hampering clinical translation of FUS and we provide guiding principles for future preclinical studies. Particularly, we focus our attention on the importance of the selection of clinically relevant animal models and to the standardization of methods for FUS delivery, which will be paramount to the successful clinical translation of this promising technology for treatment in GBM patients. We also discuss how preclinical FUS research can benefit the development of GBM immunotherapies.

1. Introduction

Glioblastoma multiforme (GBM) is one of the most aggressive and difficult to treat types of primary brain cancer, reflected in a 5-year survival rate of only 5.1% [1]. Despite incremental progress over the past 15 years, median survival time for patients undergoing standard of care treatment with debulking surgery followed by adjuvant chemo-radiation therapy remains limited to 15 months [2]. One key aspect limiting the efficacy of current treatments is the poor accumulation of systemic chemotherapeutic agents in the tumour tissue, which is significantly hampered by the presence of the blood-brain barrier (BBB) [3]. The BBB is a specialized type of vasculature characterizing the central nervous system that tightly regulates brain homeostasis to protect the brain from a broad range of harmful material. GBM is typically characterised by heterogeneous BBB integrity; the tumour core exhibits a highly disrupted and dysfunctional BBB, largely due to abnormal angiogenesis. This area of the tumour is easily visible on T1-weighted contrast enhanced MRI scans [4]. At the peripheral edge of the gross tumour mass, infiltrating tumour invading the surrounding brain is typically characterised by an intact BBB, which greatly limits the penetration of exogeneous agents into these areas of the tumour, making them “invisible” on standard MRI scans [4]. As a result of the variable BBB integrity within a single tumour, the efficacy of systemic therapeutic agents is greatly limited (Fig. 1).

Focused ultrasound (FUS), and MRI-guided focused ultrasound (MRIgFUS), has emerged as a safe and non-invasive technique to induce a temporary disruption of the BBB and selectively improve systemic drug delivery to the brain [5]. As such, FUS holds great potential to improve control of disease in GBM patients by selectively enhancing accumulation of therapeutic agents in areas of infiltrating tumour that currently receive suboptimal treatment. This characteristic makes FUS a strategic approach to improve the efficacy of current and emerging immunotherapies relying on

immune checkpoint inhibitors, which hold a great therapeutic promise, but are yet to demonstrate survival benefits in the [6]. Moreover, capitalising on FUS-induced immunomodulation via stimulation of the sterile inflammatory response may provide additional therapeutic benefits for targeted GBM immunotherapies by converting the immunosuppressive tumour environment into immunostimulatory [7].

Despite the emerging body of evidence demonstrating the therapeutic benefits of FUS in preclinical models of glioma, significantly powered, controlled clinical evaluations are lacking. In this review we discuss methodological inconsistencies that are hampering the clinical translation of FUS for the treatment of GBM, provide a commentary of preclinical studies published to date, propose guiding principles for future preclinical studies, and highlight preclinical research opportunities for FUS-assisted immunotherapies in brain tumours.

2. Blood-brain barrier opening with focused ultrasound

2.1. FUS-induced BBB opening – Physical mechanism

Low-frequency FUS is a non-invasive technique that is used to temporarily and reversibly open the BBB [8,9]. MRIgFUS works by using MRI imaging to guide the delivery of low-frequency ultrasound waves in combination with systemically administered gas-filled microbubbles (MB) to selectively disrupt the BBB [10]. The echogenic MB used for this technique are commonly used ultrasound contrast agents of 1–5 μm in diameter, composed of lipid-encapsulated perfluorocarbon gas. It is worth noting that the pressure amplitudes used to induce BBB opening with FUS are of similar magnitude to the pressures used for diagnostic ultrasound (<1.5–2 MPa) and, thus, they are considered safe for human use [11]. The physical mechanisms underlying the effect of inducing BBB opening upon excitation of the MB with ultrasound energy is still poorly understood, but the following mechanism has been proposed. The ultrasonic waves induce the MB to interact with the surrounding tissue through two main modes, stable and inertial cavitation. Stable cavitation occurs under low-pressure sonication conditions, which stimulate a repetitive pattern of contraction and expansion of MB in a stable manner [12]. This oscillation motion causes microstreaming of the fluid surrounding the MB that exerts mechanical forces on the endothelium, causing transient disruption of bonds between tight junction proteins (Fig. 2) [12,13].

Inertial cavitation occurs under high-pressure sonication conditions, which results in the abrupt collapse or disruption of the MB. This causes strong mechanical forces (e.g., shock waves and microjets) to be applied to the endothelium, causing cell membrane perforation and blood vessel permeabilization [12].

One important characteristic of this mechanical technique to modulate the brain vasculature is that the BBB opening effect remains localised in the region of targeted sonication for a period that lasts four to 24 h before the tissue reverts to the normal state [5]. The temporary and reversible aspect of the FUS-induced BBB opening makes FUS a particularly good candidate for applications in enhanced drug delivery to a number of brain pathologies, including neurodegenerative diseases, such as Parkinson's disease, Alzheimer's disease, Huntington's disease, multiple sclerosis, amyotrophic lateral sclerosis and intracranial neoplasms [11,14,15].

As previously mentioned, the vasculature of a brain tumour is structurally and physiologically heterogeneous, with angiogenic tumour regions characterised by large, abnormal, and dysfunctional vessels, and infiltrating tumour regions characterised by healthy-looking microvasculature with an intact BBB (Fig. 1). Therefore, it is unlikely that the mechanism of FUS-induced BBB opening will be consistent between healthy brain, angiogenic tumour and infiltrating tumour. While there have been a range of preclinical investigations evaluating the efficiency of FUS to induce BBB opening in healthy brain and in preclinical tumour models, to our knowledge there is no study reporting the mechanistic differences underlying the BBB opening phenomenon between the three fundamentally different brain tissues (i.e., healthy brain, angiogenic tumour and infiltrating tumour). This knowledge gap has led to several fundamental limitations to the interpretation of findings from published preclinical investigations. Research studies have hitherto been undertaken on the assumption that FUS-induced BBB opening and the consequent drug extravasation in the healthy brain or in angiogenic tumour models provides sufficient evidence to infer whether FUS can increase extravasation in infiltrating tumour tissue [[16], [17], [18], [19], [20], [21], [22]]. Therefore, a comprehensive understanding of the different molecular mechanisms leading to FUS-induced BBB opening in healthy brain, angiogenic tumour and infiltrating tumour, is critical to rationally translate FUS to clinical investigations in brain cancer.

2.2. Parameter selection for non-invasive FUS – A barrier to clinical translation

The efficiency and the mode of FUS to induce BBB opening in vivo is strongly related to the type, concentration and size distribution of the MB, and the acoustic parameters used for sonication. The optimal combination of these variables has been investigated in several preclinical studies [[23], [24], [25], [26], [27], [28]]. The main findings are summarised in a comprehensive review on the optimization of FUS-induced BBB opening by Konofagou [11]. The key message emerging from these studies is that, depending on their size distribution, each type of MB ultrasound contrast agent has a specific set of sonication parameters that should be used to achieve optimal BBB opening [23,29].

In our review of preclinical trials assessing the efficiency of FUS-induced BBB opening to increase therapeutic delivery in brain tumours, a range of in-house and commercially available (e.g., SonoVue®, Definity®, Optison®) MB contrast agents were identified, all used with different administration conditions and sonication parameters. As a result, it is challenging to compare the outcome of different preclinical studies and to predict the reproducibility of the findings using another type of MB. This is an important consideration when evaluating the potential for translation of a successful preclinical study into clinical trials. Commercial availability of the contrast agent, the patients' compatibility (tolerance) of the contrast agent, and a unified MB dose delivered to the patient need to be precisely defined in standard therapeutic protocols. Currently there is one completed clinical trial and six ongoing clinical trials in GBM patients (NCT02253212, NCT02343991, NCT03626896, NCT03712293, NCT03616860, NCT03551249, NCT03714243; clinicaltrials.gov) using three different types of therapeutic ultrasound devices, including the SonoCloud® (CarThera), ExAblate® (InSightec), and NaviFUS® (NaviFUS cooperation), either with or without chemotherapy drugs [30]. The medical device used in each of these trials requires a specific type and concentration of MB. This represents a major hurdle to the development of standard clinical protocols using FUS-induced BBB opening to enhance therapeutic treatment in patients with brain tumour. It is evident

that the standardization of the choice of medical device, MB type and dose per patient, and the sonication acoustic parameters will be paramount to the successful translation of FUS-assisted combination therapies in a clinical setting.

Despite yet limited translational implications, preclinical studies remain instrumental in providing fundamental insights into biology of FUS-mediated BBB disruption and establishing optimal treatment parameters required for clinical transition. Here we present a comprehensive review of published preclinical research for optimizing FUS-mediated drug delivery to the brain undertaken during the last two decades.

3. Review of preclinical studies for FUS-enhanced drug delivery to brain tumour

The possibility of FUS-mediated BBB opening in a preclinical model (rabbit) was first demonstrated in 2001 by Hynynen et al. [31]. Over the last 20 years, multiple studies have been published describing FUS-mediated delivery of various therapeutics in healthy and tumour-bearing animals. These studies are summarised in Table 1. We have grouped the therapeutic compounds by their size considering this to be the major limiting factor for crossing even disrupted BBB [32]. (Note: sizes of therapeutics are expressed either in molecular weights (kDa) or (hydrodynamic) radius (nm). For approximate correlation of molecular weight (kDa) and hydrodynamic radius (nm) refer to https://www.fluidic.com/toolkit/hydrodynamic-radius-converter/ with a consideration that the conversion is not linear and is highly material dependent.)

3.1. Therapeutic agents

Therapeutic agents used in preclinical studies range from small chemotherapeutic drugs to large nanoparticles, and even cells. Multiple reports have been published on FUS-mediated delivery of widely used chemotherapeutics such as: doxorubicin (DOX) [[33], [34], [35], [36], [37], [38]], BCNU (Carmustine) [[39], [40], [41], [42]], temozolomide (TMZ) [15,43], cisplatin [37], carboplatin [44], irinotecan [45] and etoposide [46,47]. FUS has been used to deliver BPA-F (10B-enriched L-4-borono-phenylalanine-fructose complex) for boron neutron capture therapy (BNCT) [48] as well as a sonosensitiser DVDMS [49] to brain tumours. The size of these therapeutic moieties ranges between 200 and 1000 Da, that roughly corresponds to the size of the gadolinium contrast agents typically used in contrast enhanced MRI to confirm BBB opening.

The next group of therapeutics are protein based biopharmaceuticals that include antibody therapeutics: trastuzumab (Herceptin) and pertuzumab [18,50,51]; the immunomodulating agent IL-12 [52]; T-DM1 (ado-trastuzumab emtansine antibody-drug conjugate) [38]; 68Ga-labeled bevacizumab (Avastin) – a humanized antiangiogenic monoclonal antibody) [19]; and radiolabelled EphA2-4B3 [53] and CD47 [54] antibodies used for diagnostic imaging of gliomas. These molecules range from ~70 kDa (IL-12) to ~150 kDa (antibodies).

The following large group of therapeutics include various formulations of nanocarriers, such as liposomes and nanoparticles. Liposomes are the most commonly used nanocarriers (~75–120 nm in size) for stabilisation and improved biodistribution of therapeutic compounds as they can be modified to target a drug to a particular site of interest, e.g. liposomal doxorubicin [33,[55], [56],

[57], [58]] (including folate-conjugated polymersomal DOX [59]), paclitaxel liposomes [60], shRNA loaded liposomes [61] as well as liposomes loaded with O6BTG-C18 – a methylguanine methyltransferase (MGMT) depleting drug for treatment of temozolomide resistant gliomas [62].

Another group comprise nanoparticle-based therapies with size range ~ 7–60 nm, where small therapeutic agents are conjugated to the surface of nanoparticles. These include gold nanoparticles (GNPs) (~7 nm) [63,64], polymeric nanoparticles [65,66] and magnetic nanoparticles (MPNs) or superparamagnetic iron oxide nanoparticles (SPION) that are used with magnetic targeting assisted delivery, some of these agents have been encapsulated or coupled to non-commercial MBs [66,67].

Finally, large therapeutic agents tested for FUS-mediated delivery comprise DNA for gene therapy [68], recombinant adeno-associated viruses (rAAV) and even NK-92 cells loaded with supermagnetic nanoparticles [69].

Though all studies show beneficial effects of FUS-mediated delivery to brain tumours, doses, times, and routes of administration vary significantly between them (see Table 1) making comparative quantitative analysis of the published studies challenging.

3.2. Preclinical neuro-oncology models

Most preclinical FUS research has been conducted on small rodents, rats and mice, both healthy and tumour bearing. Multiple models of glioma, both allogenic (originating from the same species) and xenogenic (of human origin), have already been established in these animals.

Rat models include allogenic C6, 9L and F98 gliomas, which have been extensively used in preclinical neuro-oncology research to evaluate the therapeutic efficacy of a variety of treatment agents (reviewed in [70,71]). These cell lines are implanted in the brains of immunocompetent rats (Sprague-Dawley, Wistar, Fisher). Considering the aggressive and infiltrative nature of these gliomas, treatment needs to be performed within 7–14 days post implantation. Three studies have been conducted with human HER2 positive metastatic breast carcinoma lines (BT474, MDA-MB-231, MDA-MB-361) implanted in the brains of immunocompromised athymic nude rats to mimic brain metastasis [50,51,69].

Mouse models of brain tumours are mainly xenogeneic, with human glioma cell lines inoculated in the brains of immunocompromised mice. Murine lines commonly used in these experiments are Nude (Nu/Nu) [15,19], NOD/SCID [36,53] and NOD/SCID gamma (NSG) [37,64]. The following human glioma lines have been used in preclinical research: U87 [15,19,49,60], U251 [64], GBM8401 [55,72], WK1 [53]. These glioma lines, except for WK1, are highly aggressive and reach treatment size within two weeks. Allogenic murine models include the most widely used GL261 glioma [34,54,66,73], as well as MGPP3 [46,74] and SMA-497 [62] gliomas in C57BL/6, B6-albino, or VM/Dk backgrounds.

While the majority of FUS studies have been performed on tumours implanted into deep hemisphere structures (striatum, caudate putamen, cortex), two publications [37,74] reported FUS-mediated drug delivery to brain stem, with the most recent one reporting development of brain-stem glioma model (murine pontine glioma model).

3.3. FUS technology and sonication parameters

Preclinical FUS systems vary in technical specifications and components (transducers, function generators, power amplifiers, power meters and acoustic feedback controllers etc..) and have been reviewed in detail by Ellens and Partanen [75]. For the sake of simplicity, only resonant frequencies and types of transducers have been mentioned in Table 1.

Preclinical FUS systems are predominantly equipped with single-element hemispherical (SES) transducers either in-house manufactured (IHM) or sourced from commercial suppliers, including FUS Instruments (Toronto, ON, Canada), Alpinion (Bothell, WA, USA), Imasonic (Imasonic, Besançon, France), Sonic Concepts (Sonic Concepts, Seattle, WA, USA), Parametrics (Waltham, MA, USA). The resonance frequency (RF) of the FUS transducers ranges from 0.4 to 1.7 MHz. One study reported the usage of a 6-element annular array transducer (Imasonic) that carried a passive cavitation detector [62]. McDannold et al. tested a clinical transcranial FUS system – ExAblate Neuro low-frequency device (InSightec, Haifa, Israel) [44,45]. The system is equipped with a 1024-element, 230 kHz hemispherical transducer with an integrated cavitation monitoring system (acoustic emission controller). Applied acoustic powers, as peak negative pressure amplitudes (PNP) and acoustic pressures (AP) in MPa, have been unfortunately found to vary substantially between studies.

Several studies have been performed to address FUS safety exposure levels based on MB cavitation emission feedback, i.e., reaching and maintaining stable MB cavitation while avoiding inertial cavitation that increases the likelihood of causing vascular/tissue damage [58,76]. Despite the importance of the MB emission feedback monitoring to ensure effective, replicable, and safe BBB opening, only some of the studies employed acoustic emission controllers (integrated cavitation monitoring systems) for modulation of the acoustic pressures during sonication [20,37,[44], [45], [46],48,58,63,64,74,77]. These controllers commonly include an integrated passive cavitation detector (PCD) (a hydrophone) to monitor the MB activity during sonication, and the optimal AP is selected based on detection of sub and ultra-harmonic MB emissions (as described in [76]). Sonications are commonly performed at a single or multiple sites using burst mode with burst lengths of 10 ms and a pulse repetition frequency (duty cycle) of 1 Hz over 60–120 s. Cavusoglu et al. published a comprehensive study describing a closed-loop cavitation control framework to induce BBB opening without causing macro tissue damages [78].

3.4. Microbubbles

Although MB formulations and concentrations are crucial to the success and safe use of FUS, there is a huge range of MB used in preclinical FUS studies. Most studies use clinically approved and commercially available MB with a mean diameter of 2–5 μm, including SonoVue® (Bracco, Milan, Italy), BG6895 (Bracco Suisse, Geneva, Switzerland), Lumason® (Bracco) – all sulphur hexafluoride

(SF6) lipid microspheres, Definity® (Perflutren Lipid Microsphere) (Lantheus Medical Imaging, USA) and Optison® (perfluorocarbon gas-filled albumin shells) (GE healthcare). Other studies employ various in-house manufactured microspheres [46,49,54,60,65,73] that can be loaded with treatment compounds for simultaneous delivery of treatment during the cavitation process [42,61,67,79,80]. Shell modifications have been used to improve BBB/tumour targeting, e.g. VEGF-R2 antibody coating to promote targeting to glioma microvasculature [41], des-octanoyl ghrelin conjugated MB to increase targeting to endothelial cells [59] (where MB were filled with a TGFβ1 inhibitor to facilitate BBB opening by reduction of pericyte coverage); MB coupled with boron-containing polyanion nanoparticles [66]; and folate conjugated MB to assist selective aggregation around tumour cells overexpressing the folate receptor [68].

Doses of commercially available MB have been clearly specified and thus can be compared between studies. The majority of studies use clinically recommended doses for contrast-enhanced ultrasound (e.g., Definity 20 µl/kg and Optison 50 µl/kg), although the doses vary between studies. More problematic is the use of non-commercial sources of MB in some studies where the clinically recommended doses are unknown. MB are mainly delivered as bolus IV before (up to 20 s) sonication or, particularly in studies employing cavitation detectors, continuously during sonication. Sun et al. highlighted the importance of using freshly prepared MB that are maintained in suspension during infusion. They employed a mechanical system constantly rotating the syringe to keep the MB mixed throughout their experiments [58].

Several safety studies have been performed to test and compare different MB formulations and to attempt dosage optimisations [29,81,82]. McMahon and Hynynen reported that the MB dose has a significant effect on BBB permeability, though they noted that a high MB dose may be beneficial when minimisation of tissue damage is not paramount, such as in the delivery of treatment agents to brain tumours [83]. A comprehensive review of different ultrasound contrast agents used for transient FUS-mediated BBB disruption has been recently published by Dauba et al. [84]. The review identifies the inconsistencies between published studies and discusses the challenges related to the optimal formulation of contrast agents. Another recent review by Jones and Hynynen provided a comprehensive overview of the MB oscillation dynamics, acoustic emissions, and biological effects associated with ultrasound-stimulated MB in vivo [85]. They summarised recent advances in acoustic-based strategies for the detection, control, and mapping of MB activity in the brain.

3.5. Characterisation of FUS-induced BBB opening

Many preclinical FUS studies employ T1-weighted contrast enhanced MRI with gadolinium-based contrast agents commonly used in routine clinical practice, including gadopentetate dimeglumine (Gd-DPTA) (Magnevist), Gadobutrol (Gd-DO3A-butrol) (Gadovist, Gadavist), Gadodiamide (Omniscan), and Gadoterate Meglumine (Gd-DOTA) (Dotarem) to confirm the BBB disruption after FUS. The contrast is administered either IV simultaneously or after FUS, or as an intraperitoneal bolus injection [46,74]. Several studies set out dynamic contrast enhanced (DCE)-MRI protocols to follow the dynamics of BBB opening [35,57,63]. Nevertheless, the generally used method to confirm BBB opening remains ex vivo histological assessment following IV injection of anionic dyes such as Trypan or Evans blue, alone or coupled with contrast enhanced MRI prior to animal sacrifice.

However, the nature of ex vivo assessments of FUS-induced BBB disruption makes longitudinal studies in a single animal impossible.

It is important to note that the size of the above-mentioned agents is ~900 Da and thus characterisation of BBB opening can be truly indicative only for small therapeutic agents. The delivery of larger therapeutic molecules (e.g., antibodies ~150 kDa and nanoparticles from 500 kDa (5.2 nm) and above) ideally requires another method to prove their ability to cross the BBB. Aryal et al. commented on the size mismatch between liposomal and Gd-DTPA contrast agents, highlighting that it may be necessary to use a larger MRI contrast agent to effectively evaluate the FUS-induced BBB permeability when large drug carriers, such as liposomes, are used [86]. Fluorescent-tagged dextrans with different molecular weights (3–2000 kDa) were used as treatment surrogates to mimic drug penetration following FUS-mediated BBB-opening and to investigate the influence of molecular size on BBB permeability [19,32,87]. Papachristodoulou et al. demonstrated the ability of fluorescent carbocyanine dye (DiD) labeled liposomes to extravasate following BBB disruption [62]. Radiolabelled compounds remain a valid and reliable option for BBB permeability evaluations [19,53,54], though they require a PET scanner and radiopharmaceutical facilities for on-site radioisotope synthesis that are not commonly available in research centres. Recent reviews by Saunders et al. [88]. and Ahishali and Kaya [89] discussed the advantages and the disadvantages of a large number of differently sized and charged BBB integrity markers.

3.6. Discussion of limitations and advantages of preclinical FUS

Focused ultrasound (FUS), and in particular MRIgFUS, has emerged as a safe and non-invasive technique to temporarily disrupt the BBB and selectively improve systemic drug delivery to the brain. Despite the emerging body of evidence demonstrating the therapeutic benefits of FUS in preclinical models of glioma, significantly powered, controlled clinical evaluations are lacking. The diversity of FUS systems, transducers, and treatment parameters as well as the breadth of the animal and tumour models used in FUS preclinical studies to date, has both limitations as well as advantages. This is especially evident with the three crucial FUS parameters: transducer frequency, applied acoustic pressure and microbubble type/concentration.

The single element spherical transducers used in preclinical studies range in resonance frequencies from 0.4–1.7 MHz, with higher frequency transducers having a smaller focal volume that allows targeting of smaller structures/regions in the brain. However, improved skull penetration can be achieved with lower frequency devices, making these preferable for use in larger animals and especially in clinical settings. Lower frequency sonication has also been associated with less microvasculature damage [90].

While the exact mechanisms of the BBB disruption are still not fully understood, they are presumed to be a function of interactions between the ultrasound frequency, the applied AP, the size distribution and concentration of MB, and the morphology (size/structure) of the microvasculature. The ultrasound frequency (i.e., the RF of the transducer) as well as the applied AP has a large effect on the MB cavitation threshold, with lower frequency transducers allowing the same mechanical effects to be achieved with lower APs. McDannold et al. described the mechanical index (MI) as a

meaningful metric for ultrasound-induced BBB disruption [91]. The MI is a measure of the power of an ultrasound beam that serves as an indicator for the possible adverse mechanical (i.e., non-thermal) bioeffects of the acoustic field, such as streaming and cavitation [92]. It is defined as peak negative pressure (AP in MPa) divided by the square root of the transducer frequency (MHz). The results from this study suggest that the MI threshold for BBB disruption (value where the probability for disruption was estimated to be 50%) was 0.46.

Acoustic pressures are known to depend on skull thickness, animal age and weight, and ideally should be set below the inertial MB cavitation threshold to ensure safe and steady BBB opening without tissue/vascular damage. Acoustic feedback control strategies largely minimise the damage risk [93] with the presence of a cavitation monitoring system being crucial for ensuring the safety and reproducibility of studies moving forward. Several studies have been performed to address FUS safety exposure levels based on MB cavitation emission feedback, i.e., reaching and maintaining stable MB cavitation while avoiding inertial cavitation that increases the likelihood of tissue damage [58,76,78].

Differences in MB size, concentration, infusion rates, and oxygenation states may influence the efficiency of BBB opening [94]. Even commercial MB preparations have different size distributions, dispersity and concentration (e.g. Definity: mean diameter 1.1–3.3 μm, 1.2E × 1010 MB/ml, Optison: mean diameter 2.0–4.5 μm, 5–8 × 108 MB/ml), which may impact their ability to open the BBB [94]. There is evidence that activating Definity MB at different temperatures can induce size distribution changes [95]. Using fresh MB preparations is critical as long suspension time leads to MB degradation, hence reducing their FUS efficacy. Another important consideration when using the FUS technique on small rodent brains is susceptibility to standing wave artifacts. Standing waves occur due to reflections at the boundary between the skull and the brain at low excitation frequency (< 650 kHz) and/or relatively long pulse length (> 10 ms), resulting in higher in-situ peak AP than can lead to microhemorrhages in the brain even at low APs [96,97].

It is important to note that the degree of BBB opening, and hence the size of treatment agents that can be delivered by FUS, appears to be dependent on the AP. Chen and Konofagou demonstrated that the delivery of relatively small agents (up to 70 kDa) was achieved with stable cavitation; however, inertial was associated with the successful delivery of larger molecules (500 and 2000 kDa) [32].

With regards to the treatment area and the timing of treatment, most studies (except the ones using healthy animals to assess drug delivery to brain) set FUS target points within the tumour and tumour border regions. Some apply multiple sonication separated by different time intervals [44,45,[50], [51], [52],54,60,65,98] – which reflect more clinically relevant settings, as documented in recent clinical trials where sonication was repeated up to a maximum of six times [[99], [100], [101]].

Since FUS efficiency depends on vascularisation status, it is important to keep in mind the difference in vascularisation between healthy brain, early-stage tumour, an advanced tumour with already

disrupted BBB and infiltrating tumour. This aspect which is often overlooked warrants consideration especially when using highly aggressive tumour models. Potential issues of evaluating the efficacy of FUS in commonly used aggressive glioma models are abnormal vasculature, different vascular densities, impaired blood brain tumour barrier and heterogeneously leaky microvessels [102]. Drug delivery to gliomas (especially nanoparticle-based therapies) significantly depends on the structural and functional properties of the tumour vasculature. For, instance, it has been demonstrated that FUS-mediated BBB opening was not successfully achieved in vessels over 30 μm in diameter in two preclinical glioma models [65]. These aspects pose significant limitations to the comparability of current studies and to the validation of studies where sonication is applied in regions of healthy brain or tumour with already disrupted BBB. Another caveat of the preclinical research is that most of the studies have been performed on small rodents that lack heterogeneous brain anatomy and vasculature of a human brain [103].

Given the above considerations, a methodology that allows BBB opening assessment in vivo in a non-invasive, quantitative, and clinically translatable way is paramount. Unfortunately, the majority of preclinical studies use ex vivo techniques (e.g., Evans or Trypan Blue dies) that do not provide quantitative information and are not clinically translatable. Studies using contrast enhanced-MRI mostly employ T1-weighted post-contrast anatomical imaging that provides only qualitative or semi-quantitative information (e.g., volume changes measurements). DCE-MRI (or quantitative T1 subtraction maps) has the potential to provide fully quantitative values of BBB permeability that would allow characterisation of the BBB opening window and evaluation of the relationship between BBB permeability and the size of the treatment agent. Though contrast enhanced MRI remains the gold standard for assessment of FUS-induced BBB opening, it has certain limitations for compounds above 1 kDa in size (the maximum for gadolinium-based contrast agents). The use of larger gadolinium-based molecules could be a plausible solution to this problem, while using large, radiolabelled compounds (e.g., antibodies) in combination with PET imaging could provide additional information on drug uptake, as well as biodistribution and pharmacokinetic data for the treatment agent.

Despite the significant inconsistencies in the preclinical work published to this date, preclinical FUS research provides important opportunities to optimise sonication parameters required for improved drug delivery to brain tumours, and to unravel the exact mechanisms that underpin BBB opening using FUS.

4. FUS and immunotherapies: How preclinical studies can benefit clinical therapies

4.1. FUS-induced sterile inflammation

The phenomenon of sterile inflammation or sterile inflammatory response (SIR) has been known for decades (reviewed by Rock et al.) [110]. It refers to a non-pathogen-associated inflammatory response and has been associated with various traumatic and disease states. SIR occurs in various CNS disorders (Alzheimer's, Parkinson's and Huntington's diseases, amyotrophic lateral sclerosis, epilepsy, or as a result of brain injuries, such as haemorrhage, stroke and traumatic brain injury) [111]. SIR is mediated by the innate immune system and is essential for efficient tissue repair [112].

The hallmarks of SIR in CNS are astrogliosis and microgliosis, manifested by upregulation of glial fibrillary acidic protein (GFAP) and ionized calcium binding adaptor molecule 1 (Iba1) expression – the key markers of activated astrocytes and microglia, respectively. Astroglia and microglia maintain CNS homeostasis and respond to injury by direct signalling through cytokines and other molecules [113,114]. Once activated, the microglia can further impair BBB function by modulating the expression of tight junctions, which are essential for the BBB integrity and function [115]. SIR is also manifested by activation of NFkB (Nuclear factor kappa B) pathway – a pivotal mediator of inflammatory responses – leading to expression of various proinflammatory genes (production of cytokines and chemokines) and upregulation of adhesion molecules (e.g. ICAM1 (Intercellular adhesion molecule-1)) [116].

Though SIR is an expected and obvious consequence of BBB disruption, it has only recently been considered in the context of FUS with the first studies addressing this effect published in 2017 [83,117]. Publications addressing FUS-mediated SIR effects are summarised in Table 2.

Kovacs et al. [117] published the first comprehensive study demonstrating that FUS-induced BBB disruption initiated a cascade of molecular and cellular changes consistent with the induction of SIR in the brain parenchyma compatible with ischemia or mild traumatic brain injury. The authors reported an immediate FUS-triggered inflammatory response associated with upregulation of proinflammatory cytokines, activation of the NFκB pathway and transient activation of astrocytes and microglia, presumably caused by the mechanical effects of sonication as well as by molecules entering the brain following BBB opening, such as albumin.

McMahon and Hynynen [83] confirmed the findings of Kovacs and emphasised that MB dose has a significant effect on BBB permeability, with a damaging inflammatory response observed at high MB doses with associated activation of the NFκB signalling pathway, oedema, neuronal degeneration, neutrophil infiltration and microhemorrhage. At low MB doses which still mediated BBB opening, these effects were absent, indicating that an increase in BBB permeability can be achieved without significant inflammation. The authors emphasised the importance of optimised FUS parameters to mitigate the chances of causing injury to the brain yet noted that high MB doses may be beneficial when tissue damage is not paramount, such as in the delivery of treatment agents to brain tumours. The authors noted that the FUS parameters used by Kovacs et al. might have contributed to an exaggerated inflammatory response [83]. The administered MB dose (Optison, 500 µl/kg) has previously been shown to induce significant tissue damage when used in conjugation with FUS [20].

Further, McMahon et al. [118] analysed transcriptional changes in hippocampal rat microvessels at 6 and 24 h following FUS and reported a transient inflammatory response. This response largely returned to baseline within 24 h, and only a few inflammatory markers, such as activated astrocyte marker GFAP, remained significantly upregulated at 24 h. These observed transcriptional changes were indicative of early angiogenic processes driven by the production of proinflammatory cytokines and chemokines [119]. In a follow up study McMahon et al. [120] demonstrated that blood vessel density in rat hippocampus was modestly elevated at 7 and 14 days post FUS and returned to baseline by 21 days, these findings may have relevance to the optimal frequency of repeated treatments.

Sinharay et al. [121] assessed the SIR by in vivo PET imaging with [18F]-DPA714, a biomarker of translocator protein (TSPO), a receptor upregulated in activated microglia and macrophages [122]. The [18F]-DPA-714 binding was increased in sonicated regions of the rat brains, and corresponded to areas of activation of astroglia and microglia assessed by IHC. No cumulative SIR effect was observed after multiple FUS sessions with 7 days intervals, suggesting that the inflammation was resolved between sessions. In line with previous findings, Brighi et al. [53] demonstrated substantial astrogliosis and microgliosis in FUS-targeted tumours 3 days post sonication.

Pascal et al. [96] evaluated the activation of SIR (astrogliosis and microgliosis) following FUS-mediated BBB disruption as a function of applied AP using two different MB doses. Low APs (0.15 MPa to 0.20 MPa) resulted in mild histological changes and minimal gliosis both with low and high MB doses. Higher APs resulted in more severe histological changes and SIR activation with greater increases when using higher MB doses. While the degree of contrast enhancement on MRI was moderately associated with the degree of gliosis, the presence of subharmonic acoustic emissions was strongly associated with significant histopathological changes, independent of MB dose.

In their subsequent investigation McMahon et al. [93] demonstrated upregulation of inflammatory markers ICAM1, GFAP and MCP1 (Monocyte chemoattractant protein-1) two days post-FUS, with astrogliosis still detectable at day 10, in contradiction with Sinharay et al. [121]. Treatment with dexamethasone (DEX) abrogated FUS-induced SIR effects, suggesting that DEX provides a means of modulating the duration of BBB opening that may reduce the risk of inflammation-induced tissue damage. Poon et al. [123] assessed the cellular aspect of the immune response triggered by FUS and demonstrated acute leucocyte response with neutrophils being one of the primary cell types participating in the response immediately after the onset of FUS exposure.

Chen et al. [7] recorded prolonged immunostimulation with CD4+ and CD8+ lymphocyte recruitment induced by FUS treatment with high AP, suggesting that higher FUS exposure levels have a potential to trigger a response from tumour infiltrating lymphocytes. The study provided preliminary evidence that FUS-induced immune modulation could contribute an additional therapeutic benefit by converting the immunosuppressive tumour microenvironment into an immunostimulatory one.

In summary, SIR remains a significantly understudied phenomenon in the context of FUS-induced BBB disruption. Though publications report similar findings, there is a need for further clarification. A better understanding is required into how varying treatment parameters affect the degree of neuroinflammation following opening of the BBB. Most contradictions result from diverse MB doses/types and APs, as well as different animal models (rats vs mice) used in the experimental settings. Nevertheless, it is becoming clearer that higher MB doses and APs lead to stronger SIR and tissue damage. Thus, optimal sonication parameter selection and real-time monitoring by means of an acoustic emission controller are paramount in mitigating FUS-induced neuroinflammatory effects. On the other hand, in the context of GBM treatment, activation of SIR following FUS could be potentially used to increase therapeutic benefits by creating an immunostimulatory environment. In this context it is also important to consider that significant BBB opening required for delivery of large

treatment agents can be only achieved using relatively high AP leading to inertial cavitation [32], that in its turn leads to a certain degree of tissue damage (e.g. microhemorrhage) and hence stronger SIR response.

4.2. FUS in combination with immunotherapies

Thus far, the impenetrability of the BBB has posed a great limitation to the exploration of modern immunotherapies for the treatment of brain cancers, including antibody and cell based therapies [17]. FUS has the potential to revolutionise this field of research as it provides a means to overcome this major limitation. While a few studies have investigated the efficiency of FUS to enhance antibody penetration across the BBB in healthy mice and mouse models of Alzheimer's disease [18,[124], [125], [126]], there is little evidence of studies demonstrating that FUS can enhance the accumulation of therapeutic antibodies into brain tumours [100]. Selective modulation of the permeability of the BBB for targeted antibody delivery is an effective strategy to tackle the challenge of advancing treatments for brain cancers, as it creates opportunities for investigations in anti-cancer immunotherapies [127].

Evidence supporting the notion that immunotherapy can trigger a significant anti-tumour response in GBM has fuelled research interest in therapeutic strategies involving immune-targeting checkpoint inhibitors [127,128] (Fig. 3). GBM cells are known to be poorly immunogenic, which is largely due to their ability to develop immunosuppressive adaptive mechanisms [129], including immune checkpoints, e.g. interaction between programmed cell death (PD)-1 receptor and its ligand (PD-L1) [129,130]. The interaction of PD-1, expressed by many immune cells, with PD-L1 leads to the silencing of the anti-tumour immune response and enables PD-L1-expressing tumour cells to evade immune detection by NK cells or T cells [131]. PD-L1 is highly expressed in GBM tumour cells, and there are studies showing that its level of expression is directly correlated with the tumour grade [130,132]. Thus, therapies blocking PD-1/PD-L1 in the tumour environment hold great potential as an immunotherapy for GBM, that would facilitate anti-tumour immunity [131].

There are several ongoing clinical trials of immune checkpoint blockade in glioma involving the combination of one or more immunotherapies with radio- and/or chemotherapy. A comprehensive list and evaluation of the different therapeutic strategies adopted in these clinical trials is reported in the following reviews [[129], [130], [131],[133], [134], [135]]. Unfortunately, CheckMate143 [136], the first phase III clinical trial assessing the use of the PD-1-targeting monoclonal antibody nivolumab in recurrent GBM patients, failed to improve patients overall survival (OS) [137]. In reviewing the outcome of this clinical trial, Filley et al. [138] pointed out that the presence of the BBB played a major role on the failure of this therapeutic strategy, as it prevented T cell-antibody interactions. The follow up phase III clinical trials, CheckMate498 [139] aimed at comparing the efficacy of radiotherapy plus nivolumab with that of radiotherapy plus temozolomide (as the current standard of care) in patients with MGMT-promoter-unmethylated GBM. The second follow up trial, CheckMate548 [140] was designed to explore the efficacy of the addition of nivolumab to standard-of-care chemoradiotherapy in patients with MGMT-promoter-methylated GBM. Unfortunately, CheckMate498 failed to show improvement in OS, and preliminary results indicate that CheckMate548 failed to show improvement in progression-free survival (PFS), although data to evaluate OS are yet to be analysed [135].

Although full reports of the results of the two phase III trials are yet to be published, preliminary results from these studies and the results from the CheckMate143 suggest that the presence of the BBB represents a critical limitation not only to the application of this therapeutic strategy to recurrent GBM patients, but also to the achievement of optimal agent-target interaction in the tumour microenvironment [130].

FUS could offer an effective solution to overcome several of the limitations presented as possible causes of failure of the above-discussed trials. Using FUS to temporarily disrupt the BBB would not only allow immune-stimulating agents [141], immune checkpoint inhibitors and monoclonal antibodies to more efficiently reach their target [142], but, as discussed in the previous section, it would also boost the host anti-tumour immune response by inducing SIR due to the cavitation of the MB at the tumour site [127,[143], [144], [145]].

There is substantial evidence supporting the dual positive effect of FUS-induced drug delivery and immune-modulation. A combination of FUS with targeted immunotherapies could be the next frontier of research for improving treatment for GBM. An interesting future direction in the preclinical space would be investigating the effects of combining FUS with anti-PD-L1/PD-1 antibodies on anti-tumour immune response and on survival outcome. The main challenge in exploring this area of preclinical research is the selection of an appropriate and clinically relevant animal model of glioma, which recapitulate the complexity of human GBM at the molecular, cellular and tissue level [146].

An important characteristic determining clinical relevance of animal models for preclinical investigations of new drug delivery systems and targeted therapies in GBM is the ability to reproduce the heterogeneous structural and functional properties of the BBB observed in glioma patients [147]. As discussed in the introduction and represented in Fig. 1, most human GBM have heterogeneous BBB integrity, with the core region of the tumour characterised by disrupted and leaky BBB and surrounding regions of infiltrative tumour characterised by an intact BBB [148,149], in which drug delivery is extremely limited. Having a preclinical system that allows to evaluate the ability of a new therapeutic strategy to enhance therapeutics delivery and accumulation specifically in infiltrative tumour regions is critically important to ensure that the potential efficacy of this approach is retained in clinical translation [147].

Another important aspect of preclinical models of glioma used to evaluate targeted immunotherapies is the presence of an intact immune system. Most of the existing preclinical investigations have been carried out in mouse models with a compromised immune system, to enable xenogenic tumour engraftment and development (refer to Section 3.2 and Table 1 for details). Clearly when investigating the efficacy of immunotherapies in brain tumours an immunocompetent animal model is required. In 2014 Oh et al. [150] published a review of five immunocompetent mouse models of glioma and their relative suitability as preclinical platforms for testing novel immunotherapies. In the context of GBM investigations, the syngeneic model GL261 was reported to be the most representative model, thanks to its good reproducibility and its similar stages of tumour formation and histopathological features as human GBM [151]. However, later a

study investigating the properties of the BBB of the GL261 model via MRI and histology demonstrated that this model is characterised by a complete loss of the BBB integrity as well as its glial origin (negative GFAP expression) [152].

In the last decade, increasing research effort has been focused on the development of genetically engineered mouse models (GEMMs) of GBM, with the underlying assumption that these models would be more similar to the human counterparts [153]. However, despite the significant efforts in the development of transgenic models of GBM for immunotherapy studies, there are still some practical limitations to the currently available GEMMs that need to be addressed [154,155]. These include: variability in the latency in tumour development, the development of mixed tumours with different histological grades that fail to recapitulate the features of GBM. The targeted drugs tested in these models do not necessarily have the same activity against the equivalent human target, which results in the inability to predict therapeutic outcome in patients [154,155]. These limitations highlight the need to direct future research efforts towards strategies in order to achieve greater control over tumour development with more advanced gene editing techniques (such as CRISPR/Cas9-based strategies) and to engineer 'humanized' mouse models in which murine genes and cells are replaced with their human equivalents [135,156] .

Overall, while we are still far from having an ideal preclinical glioma model for testing novel immunotherapies, a good starting point for preclinical investigations aiming at assessing the combined effect of FUS with immune checkpoint inhibitors would be to select a current GEMM model of GBM which reproduces BBB heterogeneity of human GBM. In order to guide the model selection process, an important prelude to such an investigational study would be a pilot study to characterize the structural and physiological characteristics of the BBB in current GBM GEMMs model. This currently represents an important gap in the literature.

5. Conclusion

The lack of improvements in survival outcomes in GBM patients over the last 15 years demonstrates how challenging it is to find new, effective treatment strategies to manage this aggressive disease. FUS promises to improve GBM patient survival outcomes by enhancing the delivery of current and emerging systemic therapies to regions of infiltrating tumour that are difficult to treat with current standard of care and by eliciting an anti-tumour immune response. While existing preclinical evidence demonstrates multiple therapeutic benefits of FUS in the treatment of glioma, more robust preclinical evaluations using clinically relevant models of glioma and a standardized choice of sonication parameters and MB doses are needed to successfully ensure clinical translation of such a promising technology. Further, the emerging evidence of the benefits of FUS-induced sterile inflammation and its use as a means to deliver antibody-based targeted immunotherapies across the blood brain tumour barrier open new therapeutic opportunities that are set to address current challenges in the treatment of brain tumours.

Funding sources

This research did not receive any specific grant from funding agencies in the public, commercial, or not-for-profit sectors.

References

[1] Q.T. Ostrom, H. Gittleman, J. Fulop, M. Liu, R. Blanda, C. Kromer, Y. Wolinsky, C. Kruchko, J.S. Barnholtz-Sloan, CBTRUS statistical report: primary brain and central nervous system tumors diagnosed in the United States in 2008-2012, Neuro-Oncology 17 (Suppl. 4) (2015) iv1–iv62.

[2] R. Stupp, W.P. Mason, M.J. van den Bent, M. Weller, B. Fisher, M.J. Taphoorn, K. Belanger, A.A. Brandes, C. Marosi, U. Bogdahn, J. Curschmann, R.C. Janzer, S. K. Ludwin, T. Gorlia, A. Allgeier, D. Lacombe, J.G. Cairncross, E. Eisenhauer, R. O. Mirimanoff, European Organisation for, T. Treatment of Cancer Brain, G. Radiotherapy, G. National Cancer Institute of Canada Clinical Trials, Radiotherapy plus concomitant and adjuvant temozolomide for glioblastoma, N. Engl. J. Med. 352 (2005) 987–996.

[3] G.E. Woodworth, G.P. Dunn, E.A. Nance, J. Hanes, H. Brem, Emerging insights into barriers to effective brain tumor therapeutics, Front. Oncol. 4 (2014).

[4] M. Watanabe, R. Tanaka, N. Takeda, Magnetic resonance imaging and histopathology of cerebral gliomas, Neuroradiology 34 (1992) 463–469.

[5] L. Lamsam, E. Johnson, I.D. Connolly, M. Wintermark, M. Hayden Gephart, A review of potential applications of MR-guided focused ultrasound for targeting brain tumor therapy, Neurosurg. Focus. 44 (2018) E10.

[6] S. Sanders, W. Debinski, Challenges to successful implementation of the immune checkpoint inhibitors for treatment of glioblastoma, Int. J. Mol. Sci. 21 (2020).

[7] K.T. Chen, W.Y. Chai, Y.J. Lin, C.J. Lin, P.Y. Chen, H.C. Tsai, C.Y. Huang, J. S. Kuo, H.L. Liu, K.C. Wei, Neuronavigation-guided focused ultrasound for transcranial blood-brain barrier opening and immunostimulation in brain tumors, Sci. Adv. 7 (2021).

[8] N.J. McDannold, N.I. Vykhodtseva, K. Hynynen, Microbubble contrast agent with focused ultrasound to create brain lesions at low power levels: MR imaging and histologic study in rabbits, Radiology 241 (2006) 95–106.

[9] K. Hynynen, N. McDannold, N. Vykhodtseva, F.A. Jolesz, Noninvasive MR imaging–guided focal opening of the blood-brain barrier in rabbits, Radiology 220 (2001) 640–646.
[10] F.A. Jolesz, MRI-guided focused ultrasound surgery, Annu. Rev. Med. 60 (2009) 417–430.
[11] E.E. Konofagou, Optimization of the ultrasound-induced blood-brain barrier opening, Theranostics 2 (2012) 1223–1237.
[12] H.L. Liu, C.H. Fan, C.Y. Ting, C.K. Yeh, Combining microbubbles and ultrasound for drug delivery to brain tumors: current progress and overview, Theranostics 4 (2014) 432–444.
[13] A. Rodriguez, S.B. Tatter, W. Debinski, Neurosurgical techniques for disruption of the blood–brain barrier for glioblastoma treatment, Pharmaceutics 7 (2015) 175–187.
[14] M. Aryal, N. Vykhodtseva, Y.-Z. Zhang, J. Park, N. McDannold, Multiple treatments with liposomal doxorubicin and ultrasound-induced disruption of blood–tumor and blood–brain barriers improve outcomes in a rat glioma model, J. Control. Release 169 (2013) 103–111.
[15] H.L. Liu, C.Y. Huang, J.Y. Chen, H.Y. Wang, P.Y. Chen, K.C. Wei, Pharmacodynamic and therapeutic investigation of focused ultrasound-induced blood-brain barrier opening for enhanced temozolomide delivery in glioma treatment, PLoS One 9 (2014) e114311.
[16] J. Park, Y.Z. Zhang, N. Vykhodtseva, F.A. Jolesz, N.J. McDannold, The kinetics of blood brain barrier permeability and targeted doxorubicin delivery into brain induced by focused ultrasound, J. Control. Release 162 (2012) 134–142.
[17] M. Kinoshita, N. McDannold, F.A. Jolesz, K. Hynynen, Targeted delivery of antibodies through the blood–brain barrier by MRI-guided focused ultrasound, Biochem. Biophys. Res. Commun. 340 (2006) 1085–1090.
[18] M. Kinoshita, N. McDannold, F.A. Jolesz, K. Hynynen, Noninvasive localized delivery of Herceptin to the mouse brain by MRI-guided focused ultrasoundinduced blood-brain barrier disruption, Proc. Natl. Acad. Sci. U. S. A. 103 (2006) 11719–11723.

[19] H.L. Liu, P.H. Hsu, C.Y. Lin, C.W. Huang, W.Y. Chai, P.C. Chu, C.Y. Huang, P. Y. Chen, L.Y. Yang, J.S. Kuo, K.C. Wei, Focused ultrasound enhances central nervous system delivery of bevacizumab for malignant glioma treatment, Radiology 281 (2016) 99–108.

[20] L.H. Treat, N. McDannold, N. Vykhodtseva, Y.Z. Zhang, K. Tam, K. Hynynen, Targeted delivery of doxorubicin to the rat brain at therapeutic levels using MRIguided focused ultrasound, Int. J. Cancer 121 (2007) 901–907.

[21] J. Mei, Y. Cheng, Y. Song, Y. Yang, F. Wang, Y. Liu, Z. Wang, Y. Cheng, Y. Song, Y. Yang, F. Wang, Experimental study on targeted methotrexate delivery to the rabbit brain via magnetic resonance imaging–guided focused ultrasound, J. Ultrasound Med. 28 (2009) 871–880.

[22] K. Beccaria, M. Canney, L. Goldwirt, C. Fernandez, J. Piquet, M.C. Perier, C. Lafon, J.Y. Chapelon, A. Carpentier, Ultrasound-induced opening of the bloodbrain barrier to enhance temozolomide and irinotecan delivery: an experimental study in rabbits, J. Neurosurg. 124 (2016) 1602–1610.

[23] Y.-S. Tung, F. Vlachos, J.A. Feshitan, M.A. Borden, E.E. Konofagou, The mechanism of interaction between focused ultrasound and microbubbles in blood-brain barrier opening in mice, J. Acoust. Soc. Am. 130 (2011) 3059–3067.

[24] Y.-S. Tung, F. Vlachos, J.J. Choi, T. Deffieux, K. Selert, E.E. Konofagou, In vivo transcranial cavitation threshold detection during ultrasound-induced blood–brain barrier opening in mice, Phys. Med. Biol. 55 (2010) 6141–6155.

[25] B. Baseri, J.J. Choi, Y.-S. Tung, E.E. Konofagou, Multi-modality safety assessment of blood-brain barrier opening using focused ultrasound and definity microbubbles: a short-term study, Ultrasound Med. Biol. 36 (2010) 1445–1459.

[26] F. Vlachos, Y.S. Tung, E.E. Konofagou, Permeability assessment of the focused ultrasound-induced blood–brain barrier opening using dynamic contrastenhanced MRI, Phys. Med. Biol. 55 (2010) 5451–5466.

[27] S. Wang, G. Samiotaki, O. Olumolade, J.A. Feshitan, E.E. Konofagou, Microbubble type and distribution dependence of focused ultrasound-induced blood–brain barrier opening, Ultrasound Med. Biol. 40 (2014) 130–137.

[28] J.J. Choi, J.A. Feshitan, B. Baseri, W. Shougang, T. Yao-Sheng, M.A. Borden, E.

E. Konofagou, Microbubble-size dependence of focused ultrasound-induced blood–brain barrier opening in mice in vivo, IEEE Trans. Biomed. Eng. 57 (2010) 145–154.
[29] S.K. Wu, P.C. Chu, W.Y. Chai, S.T. Kang, C.H. Tsai, C.H. Fan, C.K. Yeh, H.L. Liu, Characterization of different microbubbles in assisting focused ultrasoundinduced blood-brain barrier opening, Sci. Rep. 7 (2017) 46689.
[30] K.T. Chen, K.C. Wei, H.L. Liu, Theranostic strategy of focused ultrasound induced blood-brain barrier opening for CNS disease treatment, Front. Pharmacol. 10 (2019) 86.
[31] K. Hynynen, N. McDannold, N. Vykhodtseva, F.A. Jolesz, Noninvasive MR imaging-guided focal opening of the blood-brain barrier in rabbits, Radiology 220 (2001) 640–646.
[32] H. Chen, E.E. Konofagou, The size of blood-brain barrier opening induced by focused ultrasound is dictated by the acoustic pressure, J. Cereb. Blood Flow Metab. 34 (2014) 1197–1204.
[33] L.H. Treat, N. McDannold, Y. Zhang, N. Vykhodtseva, K. Hynynen, Improved antitumor effect of liposomal doxorubicin after targeted blood-brain barrier disruption by MRI-guided focused ultrasound in rat glioma, Ultrasound Med. Biol. 38 (2012) 1716–1725.
[34] Z. Kovacs, B. Werner, A. Rassi, J.O. Sass, E. Martin-Fiori, M. Bernasconi, Prolonged survival upon ultrasound-enhanced doxorubicin delivery in two syngenic glioblastoma mouse models, J. Control. Release 187 (2014) 74–82.
[35] J. Park, M. Aryal, N. Vykhodtseva, Y.Z. Zhang, N. McDannold, Evaluation of permeability, doxorubicin delivery, and drug retention in a rat brain tumor model after ultrasound-induced blood-tumor barrier disruption, J. Control. Release 250 (2017) 77–85.
[36] Y.L. Lin, M.T. Wu, F.Y. Yang, Pharmacokinetics of doxorubicin in glioblastoma multiforme following ultrasound-induced blood-brain barrier disruption as determined by microdialysis, J. Pharm. Biomed. 149 (2018) 482–487.
[37] S. Alli, C.A. Figueiredo, B. Golbourn, N. Sabha, M.Y. Wu, A. Bondoc, A. Luck, D. Coluccia, C. Maslink, C. Smith, H. Wurdak, K. Hynynen, M. O'Reilly, J.

T. Rutka, Brainstem blood brain barrier disruption using focused ultrasound: a demonstration of feasibility and enhanced doxorubicin delivery, J. Control. Release 281 (2018) 29–41.
[38] C.D. Arvanitis, V. Askoxylakis, Y. Guo, M. Datta, J. Kloepper, G.B. Ferraro, M. O. Bernabeu, D. Fukumura, N. McDannold, R.K. Jain, Mechanisms of enhanced drug delivery in brain metastases with focused ultrasound-induced blood-tumor barrier disruption, Proc. Natl. Acad. Sci. U. S. A. 115 (2018) E8717–E8726.
[39] H.L. Liu, M.Y. Hua, P.Y. Chen, P.C. Chu, C.H. Pan, H.W. Yang, C.Y. Huang, J. J. Wang, T.C. Yen, K.C. Wei, Blood-brain barrier disruption with focused ultrasound enhances delivery of chemotherapeutic drugs for glioblastoma treatment, Radiology 255 (2010) 415–425.
[40] C.Y. Ting, C.H. Fan, H.L. Liu, C.Y. Huang, H.Y. Hsieh, T.C. Yen, K.C. Wei, C. K. Yeh, Concurrent blood-brain barrier opening and local drug delivery using drug-carrying microbubbles and focused ultrasound for brain glioma treatment, Biomaterials 33 (2012) 704–712.
[41] C.H. Fan, C.Y. Ting, H.L. Liu, C.Y. Huang, H.Y. Hsieh, T.C. Yen, K.C. Wei, C. K. Yeh, Antiangiogenic-targeting drug-loaded microbubbles combined with focused ultrasound for glioma treatment, Biomaterials 34 (2013) 2142–2155.
[42] C.H. Fan, C.Y. Ting, Y.C. Chang, K.C. Wei, H.L. Liu, C.K. Yeh, Drug-loaded bubbles with matched focused ultrasound excitation for concurrent blood-brain barrier opening and brain-tumor drug delivery, Acta Biomater. 15 (2015) 89–101.
[43] K.C. Wei, P.C. Chu, H.Y. Wang, C.Y. Huang, P.Y. Chen, H.C. Tsai, Y.J. Lu, P.Y. Lee, I.C. Tseng, L.Y. Feng, P.W. Hsu, T.C. Yen, H.L. Liu, Focused ultrasound-induced blood-brain barrier opening to enhance temozolomide delivery for glioblastoma treatment: a preclinical study, PLoS One 8 (2013) e58995.
[44] N. McDannold, Y. Zhang, J.G. Supko, C. Power, T. Sun, C. Peng, N. Vykhodtseva, A.J. Golby, D.A. Reardon, Acoustic feedback enables safe and reliable carboplatin delivery across the blood-brain barrier with a clinical focused ultrasound system and improves survival in a rat glioma model, Theranostics 9 (2019) 6284–6299.
[45] N. McDannold, Y.Z. Zhang, J.G. Supko, C. Power, T. Sun, N. Vykhodtseva, A.

J. Golby, D.A. Reardon, Blood-brain barrier disruption and delivery of irinotecan in a rat model using a clinical transcranial MRI-guided focused ultrasound system,

Sci. Rep. Uk 10 (2020).

[46] H.J. Wei, P.S. Upadhyayula, A.N. Pouliopoulos, Z.K. Englander, X. Zhang, C.

I. Jan, J. Guo, A. Mela, Z. Zhang, T.J.C. Wang, J.N. Bruce, P.D. Canoll, N.

A. Feldstein, S. Zacharoulis, E.E. Konofagou, C.C. Wu, Focused ultrasoundmediated

blood-brain barrier opening increases delivery and efficacy of etoposide

for glioblastoma treatment, Int. J. Radiat. Oncol. Biol. Phys. 110 (2021) 539–550.

[47] Z.K. Englander, H.J. Wei, A.N. Pouliopoulos, E. Bendau, P. Upadhyayula, C.I. Jan,

E.F. Spinazzi, N. Yoh, M. Tazhibi, N.M. McQuillan, T.J.C. Wang, J.N. Bruce,

P. Canoll, N.A. Feldstein, S. Zacharoulis, E.E. Konofagou, C.C. Wu, Focused

ultrasound mediated blood-brain barrier opening is safe and feasible in a murine

pontine glioma model, Sci. Rep. 11 (2021) 6521.

[48] R.D. Alkins, P.M. Brodersen, R.N. Sodhi, K. Hynynen, Enhancing drug delivery for

boron neutron capture therapy of brain tumors with focused ultrasound, Neuro-

Oncology 15 (2013) 1225–1235.

[49] Z.K. Pi, Y.P. Huang, Y.Y. Shen, X.J. Zeng, Y.X. Hu, T. Chen, C.Y. Li, H. Yu, S.

P. Chen, X. Chen, Sonodynamic therapy on intracranial glioblastoma xenografts

using sinoporphyrin sodium delivered by ultrasound with microbubbles, Ann.

Biomed. Eng. 47 (2019) 549–562.

[50] E.J. Park, Y.Z. Zhang, N. Vykhodtseva, N. McDannold, Ultrasound-mediated

blood-brain/blood-tumor barrier disruption improves outcomes with

trastuzumab in a breast cancer brain metastasis model, J. Control. Release 163

(2012) 277–284.

[51] T. Kobus, I.K. Zervantonakis, Y. Zhang, N.J. McDannold, Growth inhibition in a

brain metastasis model by antibody delivery using focused ultrasound-mediated

blood-brain barrier disruption, J. Control. Release 238 (2016) 281–288.

[52] P.Y. Chen, H.Y. Hsieh, C.Y. Huang, C.Y. Lin, K.C. Wei, H.L. Liu, Focused

ultrasound-induced blood-brain barrier opening to enhance interleukin-12

delivery for brain tumor immunotherapy: a preclinical feasibility study, J. Transl.

Med. 13 (2015) 93.

[53] C. Brighi, L. Reid, A.L. White, L.A. Genovesi, M. Kojic, A. Millar, Z. Bruce, B. W. Day, S. Rose, A.K. Whittaker, S. Puttick, MR-guided focused ultrasound increases antibody delivery to nonenhancing high-grade glioma, Neurooncol. Adv. 2 (2020) vdaa030.
[54] N.D. Sheybani, V.R. Breza, S. Paul, K.S. McCauley, S.S. Berr, G.W. Miller, K. D. Neumann, R.J. Price, ImmunoPET-informed sequence for focused ultrasoundtargeted mCD47 blockade controls glioma, J. Control. Release 331 (2021) 19–29.
[55] F.Y. Yang, H.E. Wang, R.S. Liu, M.C. Teng, J.J. Li, M. Lu, M.C. Wei, T.T. Wong, Pharmacokinetic analysis of 111 in-labeled liposomal doxorubicin in murine glioblastoma after blood-brain barrier disruption by focused ultrasound, PLoS One 7 (2012) e45468.
[56] M. Aryal, N. Vykhodtseva, Y.Z. Zhang, J. Park, N. McDannold, Multiple treatments with liposomal doxorubicin and ultrasound-induced disruption of blood-tumor and blood-brain barriers improve outcomes in a rat glioma model, J. Control. Release 169 (2013) 103–111.
[57] M. Aryal, J. Park, N. Vykhodtseva, Y.Z. Zhang, N. McDannold, Enhancement in blood-tumor barrier permeability and delivery of liposomal doxorubicin using focused ultrasound and microbubbles: evaluation during tumor progression in a rat glioma model, Phys. Med. Biol. 60 (2015) 2511–2527.
[58] T. Sun, Y. Zhang, C. Power, P.M. Alexander, J.T. Sutton, M. Aryal, N. Vykhodtseva, E.L. Miller, N.J. McDannold, Closed-loop control of targeted ultrasound drug delivery across the blood-brain/tumor barriers in a rat glioma model, Proc. Natl. Acad. Sci. U. S. A. 114 (2017) E10281–E10290.
[59] Y.C. Chen, C.F. Chiang, S.K. Wu, L.F. Chen, W.Y. Hsieh, W.L. Lin, Targeting microbubbles-carrying TGFbeta1 inhibitor combined with ultrasound sonication induce BBB/BTB disruption to enhance nanomedicine treatment for brain tumors, J. Control. Release 211 (2015) 53–62.
[60] Y. Shen, Z. Pi, F. Yan, C.K. Yeh, X. Zeng, X. Diao, Y. Hu, S. Chen, X. Chen, H. Zheng, Enhanced delivery of paclitaxel liposomes using focused ultrasound with microbubbles for treating nude mice bearing intracranial glioblastoma xenografts, Int. J. Nanomedicine 12 (2017) 5613–5629.

[61] G. Zhao, Q. Huang, F. Wang, X. Zhang, J. Hu, Y. Tan, N. Huang, Z. Wang, Z. Wang, Y. Cheng, Targeted shRNA-loaded liposome complex combined with focused ultrasound for blood brain barrier disruption and suppressing glioma growth, Cancer Lett. 418 (2018) 147–158.

[62] A. Papachristodoulou, R.D. Signorell, B. Werner, D. Brambilla, P. Luciani, M. Cavusoglu, J. Grandjean, M. Silginer, M. Rudin, E. Martin, M. Weller, P. Roth, J.C. Leroux, Chemotherapy sensitization of glioblastoma by focused ultrasoundmediated delivery of therapeutic liposomes, J. Control. Release 295 (2019) 130–139.

[63] R.J. Diaz, P.Z. McVeigh, M.A. O'Reilly, K. Burrell, M. Bebenek, C. Smith, A. B. Etame, G. Zadeh, K. Hynynen, B.C. Wilson, J.T. Rutka, Focused ultrasound delivery of Raman nanoparticles across the blood-brain barrier: potential for targeting experimental brain tumors, Nanomedicine 10 (2014) 1075–1087.

[64] D. Coluccia, C.A. Figueiredo, M.Y.J. Wu, A.N. Riemenschneider, R. Diaz, A. Luck, C. Smith, S. Das, C. Ackerley, M. O'Reilly, K. Hynynen, J.T. Rutka, Enhancing glioblastoma treatment using cisplatin-gold-nanoparticle conjugates and targeted delivery with magnetic resonance-guided focused ultrasound, Nanomed. Nanotechnol. 14 (2018) 1137–1148.

[65] K.F. Timbie, U. Afzal, A. Date, C. Zhang, J. Song, G. Wilson Miller, J.S. Suk, J. Hanes, R.J. Price, MR image-guided delivery of cisplatin-loaded brainpenetrating nanoparticles to invasive glioma with focused ultrasound, J. Control. Release 263 (2017) 120–131.

[66] C.H. Fan, T.W. Wang, Y.K. Hsieh, C.F. Wang, Z. Gao, A. Kim, Y. Nagasaki, C. K. Yeh, Enhancing boron uptake in brain glioma by a boron-polymer/ microbubble complex with focused ultrasound, ACS Appl. Mater. Interfaces 11 (2019) 11144–11156.

[67] C.H. Fan, C.Y. Ting, H.J. Lin, C.H. Wang, H.L. Liu, T.C. Yen, C.K. Yeh, SPIOconjugated, doxorubicin-loaded microbubbles for concurrent MRI and focusedultrasound enhanced brain-tumor drug delivery, Biomaterials 34 (2013) 3706–3715.

[68] C.H. Fan, E.L. Chang, C.Y. Ting, Y.C. Lin, E.C. Liao, C.Y. Huang, Y.C. Chang, H.

L. Chan, K.C. Wei, C.K. Yeh, Folate-conjugated gene-carrying microbubbles with focused ultrasound for concurrent blood-brain barrier opening and local gene delivery, Biomaterials 106 (2016) 46–57.
[69] R. Alkins, A. Burgess, M. Ganguly, G. Francia, R. Kerbel, W.S. Wels, K. Hynynen, Focused ultrasound delivers targeted immune cells to metastatic brain tumors, Cancer Res. 73 (2013) 1892–1899.
[70] R.F. Barth, B. Kaur, Rat brain tumor models in experimental neuro-oncology: the C6, 9L, T9, RG2, F98, BT4C, RT-2 and CNS-1 gliomas, J. Neuro-Oncol. 94 (2009) 299–312.
[71] D. Giakoumettis, A. Kritis, N. Foroglou, C6 cell line: the gold standard in glioma research, Hippokratia 22 (2018) 105–112.
[72] Y.L. Lin, M.T. Wu, F.Y. Yang, Pharmacokinetics of doxorubicin in glioblastoma multiforme following ultrasound-induced blood-brain barrier disruption as determined by microdialysis, J. Pharm. Biomed. Anal. 149 (2018) 482–487.
[73] D. Ye, J. Yuan, Y. Yue, J.B. Rubin, H. Chen, Focused ultrasound-enhanced delivery of intranasally administered anti-programmed cell death-ligand 1 antibody to an intracranial murine glioma model, Pharmaceutics 13 (2021).
[74] Z.K. Englander, H.J. Wei, A.N. Pouliopoulos, E. Bendau, P. Upadhyayula, C.I. Jan, E.F. Spinazzi, N. Yoh, M. Tazhibi, N.M. McQuillan, T.J.C. Wang, J.N. Bruce, P. Canoll, N.A. Feldstein, S. Zacharoulis, E.E. Konofagou, C.C. Wu, Focused ultrasound mediated blood-brain barrier opening is safe and feasible in a murine pontine glioma model, Sci. Rep. Uk 11 (2021).
[75] N.P. Ellens, A. Partanen, Preclinical MRI-guided focused ultrasound: a review of systems and current practices, IEEE Trans. Ultrason. Ferroelectr. Freq. Control 64 (2017) 291–305.
[76] M.A. O'Reilly, K. Hynynen, Blood-brain barrier: real-time feedback-controlled focused ultrasound disruption by using an acoustic emissions-based controller, Radiology 263 (2012) 96–106.
[77] Z. Noroozian, K. Xhima, Y. Huang, B.K. Kaspar, S. Kugler, K. Hynynen, I. Aubert, MRI-guided focused ultrasound for targeted delivery of rAAV to the brain, Methods Mol. Biol. 2019 (1950) 177–197.

[78] M. Cavusoglu, J. Zhang, G.D. Ielacqua, G. Pellegrini, R.D. Signorell, A. Papachristodoulou, D. Brambilla, P. Roth, M. Weller, M. Rudin, E. Martin, J. C. Leroux, B. Werner, Closed-loop cavitation control for focused ultrasoundmediated blood-brain barrier opening by long-circulating microbubbles, Phys. Med. Biol. 64 (2019), 045012.
[79] C.Y. Ting, C.H. Fan, H.L. Liu, C.Y. Huang, H.Y. Hsieh, T.C. Yen, K.C. Wei, C. K. Yeh, Concurrent blood-brain barrier opening and local drug delivery using drug-carrying microbubbles and focused ultrasound for brain glioma treatment, Biomaterials 33 (2012) 704–712.
[80] C.H. Fan, Y.H. Cheng, C.Y. Ting, Y.J. Ho, P.H. Hsu, H.L. Liu, C.K. Yeh, Ultrasound/magnetic targeting with SPIO-DOX-microbubble complex for imageguided drug delivery in brain tumors, Theranostics 6 (2016) 1542–1556.
[81] C. Bing, Y. Hong, C. Hernandez, M. Rich, B. Cheng, I. Munaweera, D. Szczepanski, Y. Xi, M. Bolding, A. Exner, R. Chopra, Characterization of different bubble formulations for blood-brain barrier opening using a focused ultrasound system with acoustic feedback control, Sci. Rep. 8 (2018) 7986.
[82] N.A. Lapin, K. Gill, B.R. Shah, R. Chopra, Consistent opening of the blood brain barrier using focused ultrasound with constant intravenous infusion of microbubble agent, Sci. Rep. Uk 10 (2020).
[83] D. McMahon, K. Hynynen, Acute inflammatory response following increased blood-brain barrier permeability induced by focused ultrasound is dependent on microbubble dose, Theranostics 7 (2017) 3989–4000.
[84] A. Dauba, A. Delalande, H.A.S. Kamimura, A. Conti, B. Larrat, N. Tsapis, A. Novell, Recent advances on ultrasound contrast agents for blood-brain barrier opening with focused ultrasound, Pharmaceutics 12 (2020).
[85] R.M. Jones, K. Hynynen, Advances in acoustic monitoring and control of focused ultrasound-mediated increases in blood-brain barrier permeability, Br. J. Radiol. 92 (2019) 20180601.
[86] M. Aryal, N. Vykhodtseva, Y.Z. Zhang, N. McDannold, Multiple sessions of liposomal doxorubicin delivery via focused ultrasound mediated blood-brain barrier disruption: a safety study, J. Control. Release 204 (2015) 60–69.

[87] J.J. Choi, S.G. Wang, Y.S. Tung, B. Morrison, E.E. Konofagou, Molecules of various pharmacologically-relevant sizes can cross the ultrasound-induced bloodbrain barrier opening in vivo, Ultrasound Med. Biol. 36 (2010) 58–67.
[88] N.R. Saunders, K.M. Dziegielewska, K. Mollgard, M.D. Habgood, Markers for blood-brain barrier integrity: how appropriate is Evans blue in the twenty-first century and what are the alternatives? Front. Neurosci. 9 (2015) 385.
[89] B. Ahishali, M. Kaya, Evaluation of blood-brain barrier integrity using vascular permeability markers: Evans blue, sodium fluorescein, albumin-Alexa Fluor conjugates, and horseradish peroxidase, Methods Mol. Biol. 2367 (2021) 87–103.
[90] N. McDannold, N. Vykhodtseva, K. Hynynen, Effects of acoustic parameters and ultrasound contrast agent dose on focused-ultrasound induced blood-brain barrier disruption, Ultrasound Med. Biol. 34 (2008) 930–937.
[91] N. McDannold, N. Vykhodtseva, K. Hynynen, Blood-brain barrier disruption induced by focused ultrasound and circulating preformed microbubbles appears to be characterized by the mechanical index, Ultrasound Med. Biol. 34 (2008) 834-840.
[92] T. Sen, O. Tufekcioglu, Y. Koza, Mechanical index, Anatol. J. Cardiol. 15 (2015) 334–336.
[93] D. McMahon, W. Oakden, K. Hynynen, Investigating the effects of dexamethasone on blood-brain barrier permeability and inflammatory response following focused ultrasound and microbubble exposure, Theranostics 10 (2020) 1604–1618.
[94] Z.I. Kovacs, S.R. Burks, J.A. Frank, Focused ultrasound with microbubbles induces sterile inflammatory response proportional to the blood brain barrier opening: attention to experimental conditions, Theranostics 8 (2018) 2245–2248.
[95] B.L. Helfield, X. Huo, R. Williams, D.E. Goertz, The effect of preactivation vial temperature on the acoustic properties of definity (tm), Ultrasound Med. Biol. 38 (2012) 1298–1305.
[96] A. Pascal, N. Li, K.J. Lechtenberg, J. Rosenberg, R.D. Airan, M.L. James, D. M. Bouley, K.B. Pauly, Histologic evaluation of activation of acute inflammatory response in a mouse model following ultrasound-mediated blood-brain barrier using different acoustic pressures and microbubble doses, Nanotheranostics 4 (2020) 210–223.

[97] M.A. O'Reilly, Y. Huang, K. Hynynen, The impact of standing wave effects on transcranial focused ultrasound disruption of the blood-brain barrier in a rat model, Phys. Med. Biol. 55 (2010) 5251–5267.
[98] H.-L. Liu, C.-Y. Huang, J.-Y. Chen, H.-Y.J. Wang, Pharmacodynamic and therapeutic investigation of focused ultrasound- induced blood-brain barrier opening for enhanced temozolomide delivery in glioma treatment, PLoS One 9 (2014) e114311.
[99] A. Carpentier, M. Canney, A. Vignot, V. Reina, K. Beccaria, C. Horodyckid, C. Karachi, D. Leclercq, C. Lafon, J.Y. Chapelon, L. Capelle, P. Cornu, M. Sanson, K. Hoang-Xuan, J.Y. Delattre, A. Idbaih, Clinical trial of blood-brain barrier disruption by pulsed ultrasound, Sci. Transl. Med. 8 (2016), 343re342.
[100] Y. Meng, R.M. Reilly, R.C. Pezo, M. Trudeau, A. Sahgal, A. Singnurkar, J. Perry, S. Myrehaug, C.B. Pople, B. Davidson, M. Llinas, C. Hyen, Y. Huang, C. Hamani, S. Suppiah, K. Hynynen, N. Lipsman, MR-guided focused ultrasound enhances delivery of trastuzumab to Her2-positive brain metastases, Sci. Transl. Med. 13 (2021) eabj4011.
[101] S.H. Park, M.J. Kim, H.H. Jung, W.S. Chang, H.S. Choi, I. Rachmilevitch, E. Zadicario, J.W. Chang, One-year outcome of multiple blood-brain barrier disruptions with temozolomide for the treatment of glioblastoma, Front. Oncol. 10 (2020) 1663.
[102] L.G. Dubois, L. Campanati, C. Righy, I. D'Andrea-Meira, T.C. Spohr, I. Porto-Carreiro, C.M. Pereira, J. Balca-Silva, S.A. Kahn, M.F. DosSantos, A. Oliveira Mde, A. Ximenes-da-Silva, M.C. Lopes, E. Faveret, E.L. Gasparetto, V. Moura-Neto, Gliomas and the vascular fragility of the blood brain barrier, Front. Cell. Neurosci. 8 (2014) 418.
[103] S.Y. Wu, C.S. Sanchez, G. Samiotaki, A. Buch, V.P. Ferrera, E.E. Konofagou, Characterizing focused-ultrasound mediated drug delivery to the heterogeneous primate brain in vivo with acoustic monitoring, Sci. Rep. 6 (2016) 37094.
[104] H.-L. Liu, M.-Y. Hua, P.-Y. Chen, P.-C. Chu, C.-H. Pan, H.-W. Yang, C.-Y. Huang, J.-J. Wang, T.-C. Yen, K.-C. Wei, Blood-brain barrier disruption with focused ultrasound enhances delivery of chemotherapeutic drugs for glioblastoma

treatment, Radiology 255 (2010) 415–425.
[105] K.-C. Wei, P.-C. Chu, H.-Y.J. Wang, C.-Y. Huang, P.-Y. Chen, H.-C. Tsai, Y.-J. Lu, P.-Y. Lee, I.C. Tseng, L.-Y. Feng, P.-W. Hsu, T.-C. Yen, H.-L. Liu, C. Tsai, Y.-J. Lu, P.-Y. Lee, I.C. Tseng, L.-Y. Feng, P.-W. Hsu, T.-C. Yen, Focused ultrasound-induced blood-brain barrier opening to enhance temozolomide delivery for glioblastoma treatment: a preclinical study, PLoS One 8 (2013) e58995.
[106] Z. Pi, Y. Huang, Y. Shen, X. Zeng, Y. Hu, T. Chen, C. Li, H. Yu, S. Chen, X. Chen, Sonodynamic therapy on intracranial glioblastoma xenografts using sinoporphyrin sodium delivered by ultrasound with microbubbles, Ann. Biomed. Eng. 47 (2019) 549–562.
[107] H.-L. Liu, P.-H. Hsu, C.-Y. Lin, C.-Y.C.-W. Huang, W.-Y. Chai, P.-C. Chu, C.-Y.C.-W. Huang, P.-Y. Chen, L.-Y. Yang, J.S. Kuo, K.-C. Wei, C.-Y. Hunag, P.-Y. Chen, L.-Y. Yang, J.S. Kuo, K.-C. Wei, Focused ultrasound enhances central nervous system delivery of bevacizumab for malignant glioma treatment, Radiology 281 (2016) 99–108.
[108] P.Y. Chen, H.L. Liu, M.Y. Hua, H.W. Yang, C.Y. Huang, P.C. Chu, L.A. Lyu, I. C. Tseng, L.Y. Feng, H.C. Tsai, S.M. Chen, Y.J. Lu, J.J. Wang, T.C. Yen, Y.H. Ma, T. Wu, J.P. Chen, J.I. Chuang, J.W. Shin, C. Hsueh, K.C. Wei, Novel magnetic/ ultrasound focusing system enhances nanoparticle drug delivery for glioma treatment, Neuro-Oncology 12 (2010) 1050–1060.
[109] H.L. Liu, M.Y. Hua, H.W. Yang, C.Y. Huang, P.C. Chu, J.S. Wu, I.C. Tseng, J. J. Wang, T.C. Yen, P.Y. Chen, K.C. Wei, Magnetic resonance monitoring of focused ultrasound/magnetic nanoparticle targeting delivery of therapeutic agents to the brain, Proc. Natl. Acad. Sci. U. S. A. 107 (2010) 15205–15210.
[110] K.L. Rock, E. Latz, F. Ontiveros, H. Kono, The sterile inflammatory response, Annu. Rev. Immunol. 28 (2010) 321–342.
[111] M. Banjara, C. Ghosh, Sterile Neuroinflammation and strategies for therapeutic intervention, Int. J. Inflamm. 2017 (2017) 8385961.
[112] D.J. DiSabato, N. Quan, J.P. Godbout, Neuroinflammation: the devil is in the details, J. Neurochem. 139 (2016) 136–153.
[113] S. Bachiller, I. Jimenez-Ferrer, A. Paulus, Y. Yang, M. Swanberg, T. Deierborg,

A. Boza-Serrano, Microglia in neurological diseases: a road map to brain-disease dependent-inflammatory response, Front. Cell. Neurosci. 12 (2018) 488.
[114] E. Colombo, C. Farina, Astrocytes: key regulators of neuroinflammation, Trends Immunol. 37 (2016) 608–620.
[115] A.C. da Fonseca, D. Matias, C. Garcia, R. Amaral, L.H. Geraldo, C. Freitas, F. R. Lima, The impact of microglial activation on blood-brain barrier in brain diseases, Front. Cell. Neurosci. 8 (2014) 362.
[116] T. Liu, L. Zhang, D. Joo, S.C. Sun, NF-kappaB signaling in inflammation, Signal Transduct. Target. Ther. 2 (2017).
[117] Z.I. Kovacs, S. Kim, N. Jikaria, F. Qureshi, B. Milo, B.K. Lewis, M. Bresler, S. R. Burks, J.A. Frank, Disrupting the blood-brain barrier by focused ultrasound induces sterile inflammation, Proc. Natl. Acad. Sci. U. S. A. 114 (2017) E75–E84.
[118] D. McMahon, R. Bendayan, K. Hynynen, Acute effects of focused ultrasoundinduced increases in blood-brain barrier permeability on rat microvascular transcriptome, Sci. Rep. 7 (2017) 45657.
[119] A. Naldini, F. Carraro, Role of inflammatory mediators in angiogenesis, Curr. Drug Targets Inflamm. Allergy 4 (2005) 3–8.
[120] D. McMahon, E. Mah, K. Hynynen, Angiogenic response of rat hippocampal vasculature to focused ultrasound-mediated increases in blood-brain barrier permeability, Sci. Rep. 8 (2018) 12178.
[121] S. Sinharay, T.W. Tu, Z.I. Kovacs, W. Schreiber-Stainthorp, M. Sundby, X. Zhang, G.Z. Papadakis, W.C. Reid, J.A. Frank, D.A. Hammoud, In vivo imaging of sterile microglial activation in rat brain after disrupting the blood-brain barrier with pulsed focused ultrasound: [18F]DPA-714 PET study, J. Neuroinflammation 16 (2019) 155.
[122] D.A. Hammoud, Molecular imaging of inflammation: current status, J. Nucl. Med. 57 (2016) 1161–1165.
[123] C. Poon, C. Pellow, K. Hynynen, Neutrophil recruitment and leukocyte response following focused ultrasound and microbubble mediated blood-brain barrier treatments, Theranostics 11 (2021) 1655–1671.
[124] S.B. Raymond, L.H. Treat, J.D. Dewey, N.J. McDannold, K. Hynynen, B.J. Bacskai,

Ultrasound enhanced delivery of molecular imaging and therapeutic agents in Alzheimer's disease mouse models, PLoS One 3 (2008) e2175.
[125] J.F. Jord˜ao, C.A. Ayala-Grosso, K. Markham, Y. Huang, R. Chopra, J. McLaurin, K. Hynynen, I. Aubert, Antibodies targeted to the brain with image-guided focused ultrasound reduces amyloid-β plaque load in the TgCRND8 mouse model of Alzheimer's disease, PLoS One 5 (2010) e10549.
[126] P.W. Janowicz, G. Leinenga, J. G¨otz, R.M. Nisbet, Ultrasound-mediated bloodbrain barrier opening enhances delivery of therapeutically relevant formats of a tau-specific antibody, Sci. Rep. Uk 9 (2019) 9255.
[127] O. Cohen-Inbar, Z. Xu, J.P. Sheehan, Focused ultrasound-aided immunomodulation in glioblastoma multiforme: a therapeutic concept, J. Ther. Ultrasound 4 (2016) 2.
[128] D.M. Pardoll, The blockade of immune checkpoints in cancer immunotherapy, Nat. Rev. Cancer 12 (2012) 252–264.
[129] B. Huang, H. Zhang, L. Gu, B. Ye, Z. Jian, C. Stary, X. Xiong, Advances in immunotherapy for glioblastoma multiforme, J Immunol Res 2017 (2017) 3597613.
[130] S. Xue, M. Hu, V. Iyer, J. Yu, Blocking the PD-1/PD-L1 pathway in glioma: a potential new treatment strategy, J. Hematol. Oncol. 10 (2017) 81.
[131] W. Ma, B.M. Gilligan, J. Yuan, T. Li, Current status and perspectives in translational biomarker research for PD-1/PD-L1 immune checkpoint blockade therapy, J. Hematol. Oncol. 9 (2016) 47.
[132] J. Grosso, D. Inzunza, Q. Wu, J. Simon, P. Singh, X. Zhang, T. Phillips, P. Simmons, J. Cogswell, Programmed death-ligand 1 (PD-L1) expression in various tumor types, J. Immunother. Cancer 1 (2013) P53.
[133] J. Huang, F. Liu, Z. Liu, H. Tang, H. Wu, Q. Gong, J. Chen, Immune checkpoint in glioblastoma: promising and challenging, Front. Pharmacol. 8 (2017) 242.
[134] T. McGranahan, K.E. Therkelsen, S. Ahmad, S. Nagpal, Current state of immunotherapy for treatment of glioblastoma, Curr. Treat. Options in Oncol. 20 (2019) 24.
[135] B. Weenink, P.J. French, P.A.E. Sillevis Smitt, R. Debets, M. Geurts,

Immunotherapy in glioblastoma: current shortcomings and future perspectives, Cancers 12 (2020) 751.
[136] A Study of the Effectiveness and Safety of Nivolumab Compared to Bevacizumab and of Nivolumab with or without Ipilimumab in Glioblastoma Patients (CheckMate 143), in, 2021.
[137] D.A. Reardon, A. Omuro, A.A. Brandes, J. Rieger, A. Wick, J. Sepulveda, S. Phuphanich, P. de Souza, M.S. Ahluwalia, M. Lim, G. Vlahovic, J. Sampson, OS10.3 randomized phase 3 study evaluating the efficacy and safety of nivolumab vs bevacizumab in patients with recurrent glioblastoma: CheckMate 143, Neuro-Oncology 19 (2017) iii21.
[138] A.C. Filley, M. Henriquez, M. Dey, Recurrent glioma clinical trial, CheckMate-143: the game is not over yet, Oncotarget 8 (2017) 91779–91794.
[139] An Investigational Immuno-Therapy Study of Nivolumab Compared to Temozolomide, Each Given with Radiation Therapy, for Newly-Diagnosed Patients with Glioblastoma (GBM, a Malignant Brain Cancer) (CheckMate 498), in, 2021.
[140] An Investigational Immuno-Therapy Study of Temozolomide Plus Radiation Therapy with Nivolumab or Placebo, for Newly Diagnosed Patients with Glioblastoma (GBM, a Malignant Brain Cancer) (CheckMate 548), in, 2021.
[141] P.-Y. Chen, H.-Y. Hsieh, C.-Y. Huang, C.-Y. Lin, K.-C. Wei, H.-L. Liu, Focused ultrasound-induced blood–brain barrier opening to enhance interleukin-12 delivery for brain tumor immunotherapy: a preclinical feasibility study, J. Transl. Med. 13 (2015) 93.
[142] C.T. Curley, N.D. Sheybani, T.N. Bullock, R.J. Price, Focused ultrasound immunotherapy for central nervous system pathologies: challenges and opportunities, Theranostics 7 (2017) 3608–3623.
[143] K.-T. Chen, K.-C. Wei, H.-L. Liu, Theranostic strategy of focused ultrasound induced blood-brain barrier opening for CNS disease treatment, Front. Pharmacol. 10 (2019) 86
[144] Z.I. Kovacs, S. Kim, N. Jikaria, F. Qureshi, B. Milo, B.K. Lewis, M. Bresler, S. R. Burks, J.A. Frank, Disrupting the blood-brain barrier by focused ultrasound

induces sterile inflammation, Proc. Natl. Acad. Sci. U. S. A. 114 (2017) E75–E84.
[145] J.F. Jord˜ao, E. Th´evenot, K. Markham-Coultes, T. Scarcelli, Y.-Q. Weng, K. Xhima, M. O'Reilly, Y. Huang, J. McLaurin, K. Hynynen, I. Aubert, Amyloid-β plaque reduction, endogenous antibody delivery and glial activation by brain-targeted, transcranial focused ultrasound, Exp. Neurol. 248 (2013) 16–29.
[146] J. Rossmeisl, Maximizing local access to therapeutic deliveries in glioblastoma. Part V: Clinically relevant model for testing new therapeutic approaches, in: S. De Vleeschouwer (Ed.), Glioblastoma, 2017. Brisbane (AU).
[147] C. Brighi, L. Reid, L.A. Genovesi, M. Kojic, A. Millar, Z. Bruce, A.L. White, B. W. Day, S. Rose, A.K. Whittaker, S. Puttick, Comparative study of preclinical mouse models of high-grade glioma for nanomedicine research: the importance of reproducing blood-brain barrier heterogeneity, Theranostics 10 (2020) 6361–6371.
[148] J.N. Sarkaria, L.S. Hu, I.F. Parney, D.H. Pafundi, D.H. Brinkmann, N.N. Laack, C. Giannini, T.C. Burns, S.H. Kizilbash, J.K. Laramy, K.R. Swanson, T. J. Kaufmann, P.D. Brown, N.Y.R. Agar, E. Galanis, J.C. Buckner, W.F. Elmquist, Is the blood-brain barrier really disrupted in all glioblastomas? A critical assessment of existing clinical data, Neuro-Oncology 20 (2018) 184–191.
[149] M.S. McHenry, K.A. Balogun, B.C. McDonald, R.C. Vreeman, E.C. Whipple, L. Serghides, In utero exposure to HIV and/or antiretroviral therapy: a systematic review of preclinical and clinical evidence of cognitive outcomes, J. Int. AIDS Soc. 22 (2019) e25275.
[150] T. Oh, S. Fakurnejad, E.T. Sayegh, A.J. Clark, M.E. Ivan, M.Z. Sun, M. Safaee, O. Bloch, C.D. James, A.T. Parsa, Immunocompetent murine models for the study of glioblastoma immunotherapy, J. Transl. Med. 12 (2014) 1–10.
[151] T. Szatm´ari, K. Lumniczky, S. D´esaknai, S. Trajcevski, E.J. Hídv´egi, H. Hamada, G. S´afr´any, Detailed characterization of the mouse glioma 261 tumor model for experimental glioblastoma therapy, Cancer Sci. 97 (2006) 546–553.
[152] C. Leten, T. Struys, T. Dresselaers, U. Himmelreich, In vivo and ex vivo assessment of the blood brain barrier integrity in different glioblastoma animal models, J. Neuro-Oncol. 119 (2014) 297–306.

[153] A.T. Yeo, A. Charest, Immune checkpoint blockade biology in mouse models of glioblastoma, J. Cell. Biochem. 118 (2017) 2516–2527.

[154] K. Lenting, R. Verhaak, L. Pieter, W. Leenders, Glioma: experimental models and reality, Acta Neuropathol. 133 (2017) 263–282.

[155] L. Zitvogel, J.M. Pitt, R. Daill`ere, M.J. Smyth, G. Kroemer, Mouse models in oncoimmunology, Nat. Rev. Cancer 16 (2016) 759–773.

[156] O. Kepp, A. Marabelle, L. Zitvogel, G. Kroemer, Oncolysis without viruses - inducing systemic anticancer immune responses with local therapies, Nat. Rev. Clin. Oncol. 17 (2020) 49–64.

Figure Captions

Fig. 1. Drug delivery across the blood-brain barrier in glioma. Post-contrast T1-weighted MRI image of a glioblastoma patient, showing areas of contrast enhancement characterised by a disrupted blood-brain barrier, which allows drug penetration and accumulation into the tumour. Peritumoural areas next to the contrast enhancing lesion are likely characterised by infiltrating tumour with an intact blood-brain barrier, which prevents effective drug delivery to the tumour.

Fig. 2. Mechanism of action of focused ultrasound. Gas filled microbubbles are injected intravenously. Upon sonication of the targeted areas the microbubbles initiate stable cavitation. The microbubbles expansion, the radiative force, and the flow of liquid around the microbubbles (microstreaming) caused by the ultrasound waves result in shear stress applied to the cells membrane that ultimately leads to a temporary disruption of the blood-brain barrier. Adapted from "Blood Brain Barrier", by BioRender.com (2021). Retrieved from https://app.biorender.com/biorender-templates.

Fig. 3. Targeting brain tumours with immune checkpoint inhibitors. Temporary disruption of the blood-brain barrier allows immune checkpoint inhibitors (anti PD-1 antibodies) to leak into the

extravascular space and target immune checkpoints (PD-1 receptors) expressed on T cells. The link of the immune checkpoint inhibitors to PD-1 activates T cells, preventing the interaction between PD-1 and PD-L1 receptors expressed on tumour cells, which normally silences the anti-tumour immune response and enables PD-L1-expressing tumour cells to evade immune detection by T cells. Adapted from “Blood Brain Barrier” and “Immune Checkpoint Inhibitor Against Tumour Cell”, by BioRender.com (2021). Retrieved from https://app.biorender.com/biorender-templates.

Fig 1

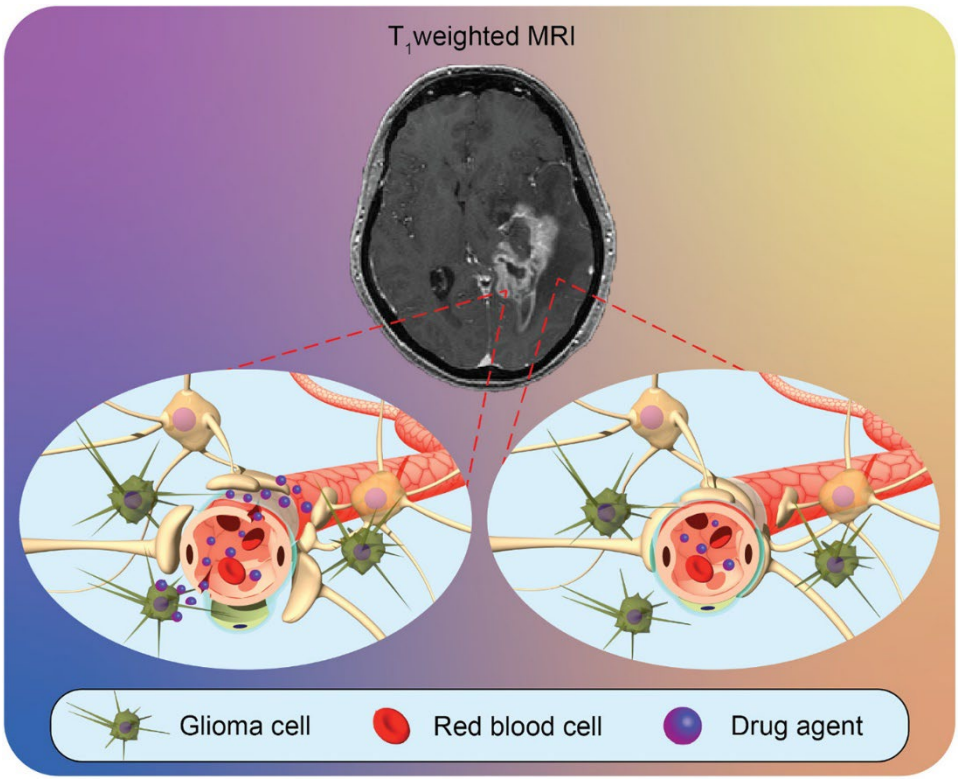

Fig 2

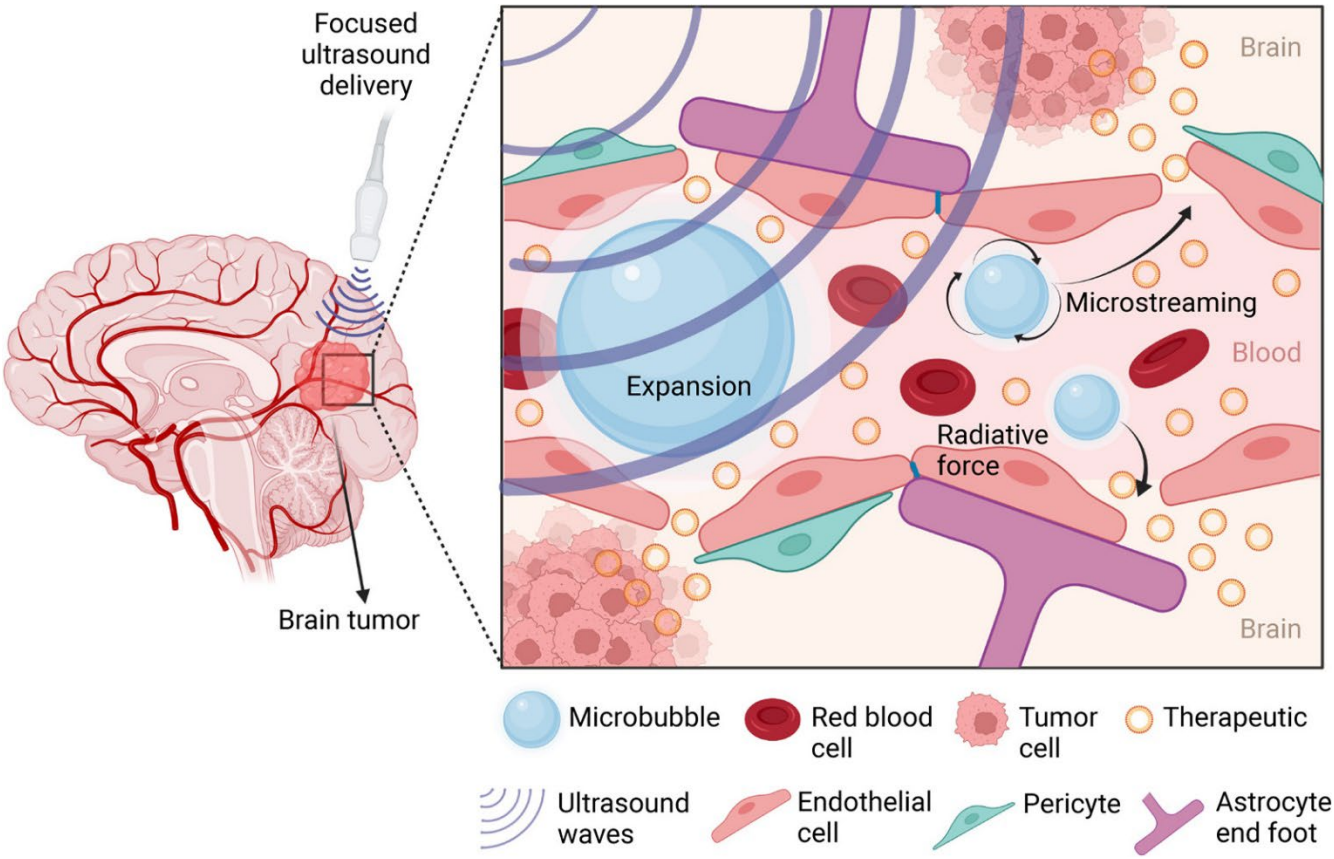

Fig 3

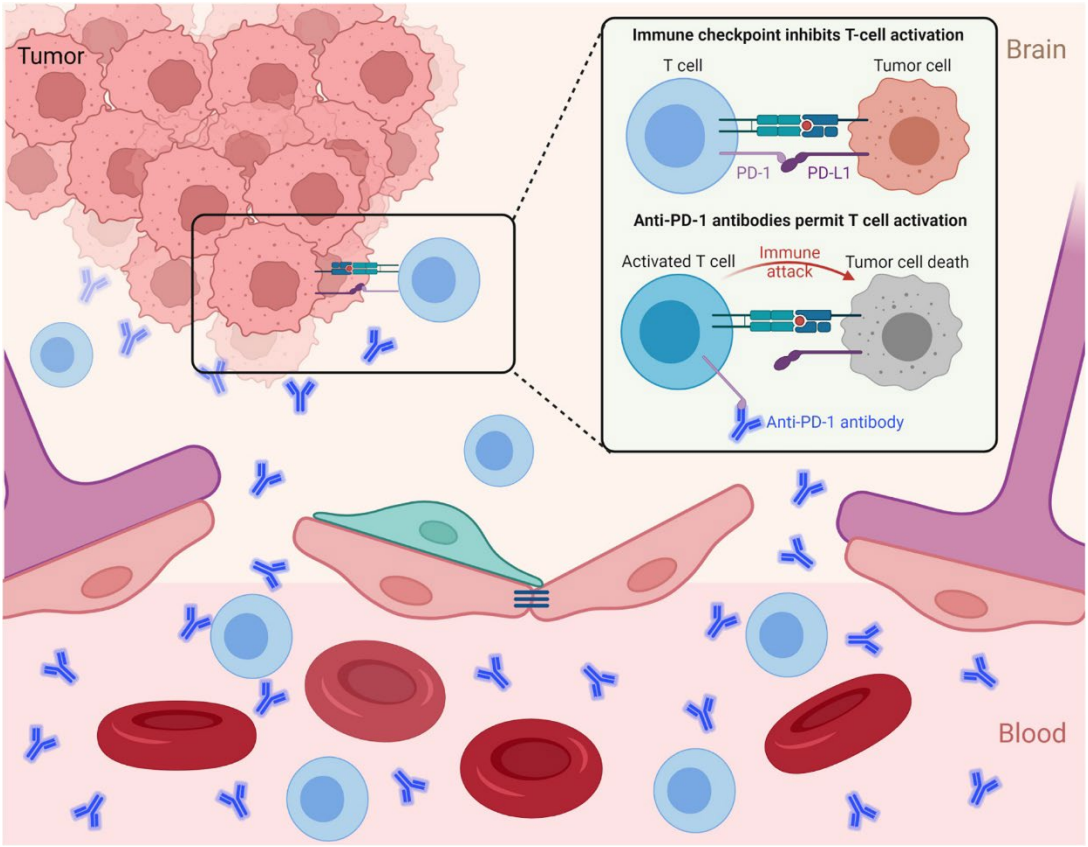

Graphical Abstract

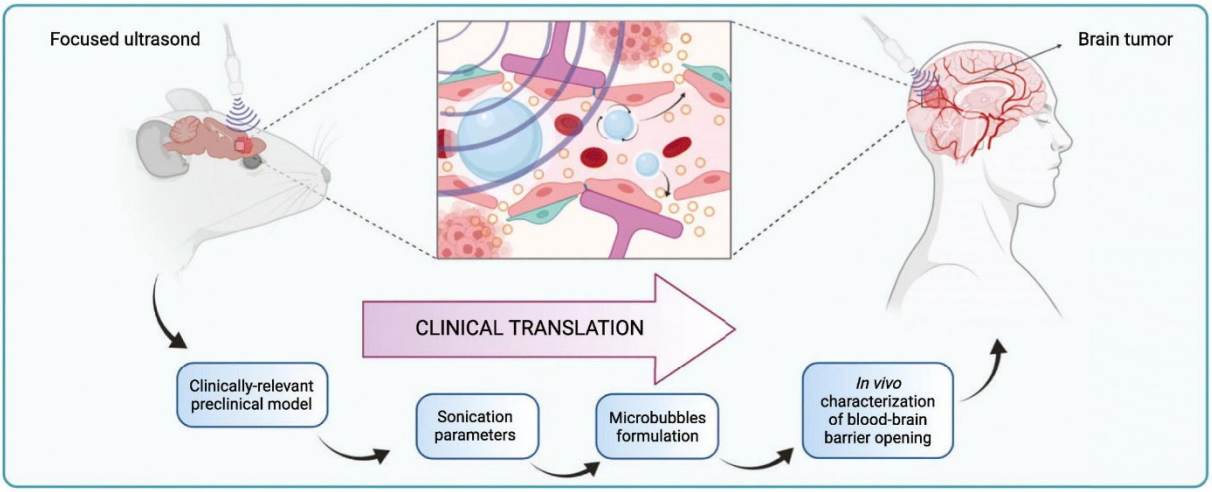
Focused ultrasond
Brain tumor
CLINICAL TRANSLATION
Clinically-relevant preclinical model
Sonication parameters
Microbubbles formulation
In vivo characterization of blood-brain barrier opening

Table 1
Preclinical studies investigating FUS-mediated drug delivery to the brain.

Reference	Treatment size	Dose and method of delivery	Animal model Tumour model Implantation site	FUS technology Sonication parameters	Microbubbles	Method to characterize BBB disruption	Findings
Small therapeutic compounds (<1000 Da)							
Treat 2007 [20]	Doxorubicin (DOX) 543 Da	3.0–5.7 mg/kg IV after FUS	Sprague-Dawley rats healthy	SES FUS transducer (IHM): RF 1.5 or 1.7 MHz BL 10 ms; RF 1 Hz; T 30–120 s AP 0.36–2.5 MPa (1.1 MPa for DOX delivery)	Optison 50–500 µl/kg (optimal 100 µl/kg)	(1) CE MRI: Gd-DTPA 0.125 mmol/kg; (2) TB, 80 mg/kg, IV after sonication	Different sonication parameters and MB concentrations tested. Optison at 100 µl/kg resulted in a 3.5-fold increase in DOX concentrations in the brain with minimal tissue effects. Higher Optison dose resulted in 21-fold increase in DOX concentrations with significant tissue damage
Liu 2010 [104]	Carmustine (BCNU) 241 Da	13.5 mg/kg IV after FUS	Sprague-Dawley rats C6 rat glioma striatum	SES FUS transducer (Imasonics): RF 400 kHz BL 10 ms; PRF 1 Hz; T 30 s AP 0.62 MPa	SonoVue, 2.5 µg/kg bolus before sonication	(1) CE MRI: Gd-DPTA (Magnevist), 0.25 ml/kg, (2) EB, IV before sonication	FUS enhanced the penetration of BCNU through the BBB by 202% in tumour targeted regions and improved animal survival by 85.9% relative to untreated controls
Ting 2012 [40]	Carmustine (BCNU) 241 Da	1.25 mg/animal (~4–5 mg/kg) MB loaded	Sprague-Dawley rats C6 rat glioma striatum	SES FUS transducer (V302, Panametrics): RF 1 MHz BL 10 ms; PRF 5 Hz; T 120 s AP 0.7 MP (over two sonication sites)	IHM lipid MB BCNU loaded, 0.5 ml/animal	EB, 100 mg/kg, IV 5 min before sonication	Encapsulation of BCNU in MBs prolonged its circulatory half-life by 5-fold, reduced liver uptake by 5-fold. BCNU-MB with FUS controlled tumour progression and improved median survival
Alkins 2013 [48]	BPA-F (Borono-phenylalanine-Fructose) ~500 Da	250 mg/kg	Fisher rats 9L rat glioma frontal striatum	SES FUS transducer (IHM): RF 558 kHz BL 10 ms; PRF 1 Hz; T 120 AP 0.4 MPa	Definity, 20 µl/kg	CE MRI: Gadodiamide (Omniscan), 0.2 ml/kg	Boron neutron capture therapy (BNCT) of glioblastoma. FUS increased the accumulation of Boron-^{10}B in the main tumour and infiltrating cells
Wei 2013 [105]	Temozolomide (TMZ) 194 Da	75 mg/kg/day for 5 days by gavage with FUS on day 1 and 3	Fisher rats 9L rat glioma striatum	SES FUS transducer (Imasonics): RF 500 kHz BL 10 ms; PRF1 Hz; T 60 s AP 0.6 MPa	SonoVue, 100 µl/kg	(1) CE MRI: Gd-DPTA (Magnevist), 0.1 mmol/kg IV before FUS; (2) EB, 2 mg/kg	FUS-mediated BBBD increased the local concentration of TMZ reduced the 7-day tumour progression and extended median animal survival
Fan 2013 [41]	Carmustine (BCNU) 241 Da Drug-loaded MB coupled to VEGF-R2 Ab for antiangiogenic targeting	1.25 mg/animal (~4–5 mg/kg) MB loaded	Sprague-Dawley rats C6 rat glioma striatum	SES FUS transducer: (V302, Panametrics): RF 1 MHz BL 10 ms, PRF 5 Hz, T 120 s AP 0.7 MP	IHM lipid MB BCNU loaded coated with VEGF-R2 antibody 0.5 ml/animal	EB, 100 mg/kg, IV 5 min before sonication	Angiogenic-targeting of BCNU drug-loaded MBs directed to regions of tumour vasculature significantly enhanced the targeted drug release and reduced tumour progression
Liu 2014 [98]	Temozolomide (TMZ) 194 Da	2.5, 5 and 25 mg/kg/day for 3 days by gavage 10	Nude (NU/NU) mice U87 human glioma striatum	SES FUS transducer (Sonic Concepts): RF 500 kHz BL 10 ms; PRF 1 Hz; T 60 s AP 0.3–0.7 MPa	SonoVue, 4 µl/mouse	EB, 4 µl/mouse	FUS-BBBD increased local concentration of orally administered TMZ improving the control of tumour progression and animal survival

Table 1 (*continued*)

Reference	Treatment size	Dose and method of delivery	Animal model Tumour model Implantation site	FUS technology Sonication parameters	Microbubbles	Method to characterize BBB disruption	Findings
Kovacs 2014 [34]	Doxorubicin (DOX) 543 Da	8 mg/kg single dose IV before FUS	B6-albino mice GL261 mouse glioma right striatum	SES FUS transducer (H-107MR, Sonic Concepts): RF 612.5 kHz BL 10 ms; PRF1 Hz; T 60 s AP 0.4 MPa	BG6895, 60 µl/ mouse 1 µl/s during sonication	(1) CE-MRI: gadodiamide (Omniscan), 0.2 mmol/ kg; (2) EB, 50 µl/mouse before sonication	DOX + FUS-mediated BBBD significantly increased survival and slowed disease progression in syngeneic GBM mouse model
Fan 2015 [42]	Carmustine (BCNU) 241 Da	Drug-loaded MB dose not specified	Sprague-Dawley rats C6 rat glioma striatum	SES FUS transducers: (1) V302, Panametrics: RF 1 MHz; (2) SU-110, Sonic Concepts: RF 10 MHz PRF 10 Hz, T 4 min AP 0.5–4.5 MPa	IHM lipid MB, BCNU loaded, 0.5E+0.9 MB/ animal, 20 s before sonication	EB, 100 mg/kg IV 5 min before sonication	FUS-mediated treatment with BCNU-loaded MB resulted in significant improvement in BCNU delivery to the brain, reduction of tumour progression and improved median survival
Park 2017 [35]	Doxorubicin (DOX) 543 Da	5.67 mg/kg IV after FUS	Sprague–Dawley rats 9L rat glioma cerebral cortex	SES FUS transducer (IHM): RF 690 kHz BL 10 ms; PRF 1 Hz; T 60 s AP 0.68–0.72 MPa	Definity, 10 µl/kg bolus at start of sonication	(1) DCE-MRI: Gd-DPTA (Magnevist), 0.25 mmol/kg IV after FUS; (2) TB, 0.1 g/kg	FUS increased DOX delivery across the BBB and blood-tumour-barrier. DOX was retained in the tissue at significantly enhanced levels for at least 24 h
Lin 2018 [72]	Doxorubicin (DOX) 543 Da	5 mg/kg IV before FUS with MBs	NOD/SCID mice GBM8401 human glioma left hemisphere	SES FUS transducer (A392S, Panametrics): RF 1.0 MHz, BL 50 ms; PRF 1 Hz; T 60 s AP 2.86 W	Sonovue, 0.3 ml/ kg bolus before sonication	DOX microdialisis in the tumour as readout	FUS-mediated BBBD resulted in 2.35-fold increase in tumour-to-normal brain DOX ratio
Alli 2018 [37]	Cisplatin 301 Da Doxorubicin (DOX) 543 Da	Rats: 1.5 mg/ kg cisplatin; Mice: 5 mg/ kg DOX IV bolus at the time of FUS	Sprague-Dawley rats NSG mice healthy brain stem (pons)	SES FUS transducer (IHM): RF 1.68 MHz BL 10 ms; PRF 1 Hz, T 120 min AP 1.1 ± 0.3 MPa (rats); 0.71 ± 0.15 MPa (mice) Acoustic emission feedback	Definity, 20 µl/kg bolus at start of sonication	(1) CE-MRI: Gadobutrol (Gadovist), 0.1 ml/kg, after FUS; (2) EB, 4 ml/kg of 4% solution after CE-MRI	Demonstration of pre-clinical feasibility of FUS-mediated drug delivery in pons, opening possibilities for treatment of brain stem tumours with intact BBB, e.g. diffuse Intrinsic Pontine Glioma (DIPG)
Arvanitis 2018 [38]	Doxorubicin (DOX) 543 Da	7.5 mg/kg IV after FUS	mice BT474 human breast carcinoma	SES FUS transducer (IHM): RF 1.025 MHz. BL 10 ms, PRF 1 Hz, T 120 min AP 0.48 MPa	Definity, 20 µl/kg during sonication	Intravital multiphoton microscopy (pharmacokinetics and intratumoural uptake of DOX)	FUS improved DOX in brain metastasis. Significant increases DOX extravasation (7-fold) and penetration (>100 vs. <20 µm) after the application of FUS. Significantly enhanced endothelial cell uptake and transvascular transport based on physiologically based pharmacokinetic (PBPK) modelling
Pi 2019 [106]	Sinoporphyrin sodium (DVDMS) ~1,2 kDa	2 mg/kg IV with MBs	Balb/c nude mice U87 human glioma striatum	SES FUS transducer (IHM): RF 0.996 MHz BL 10 ms, PRF 1 Hz, T 60 s AP 0.64 MPa	IHM MBs, 0.2 µl/g, 15 s before sonication	DVDMS fluorescence	FUS-mediated delivery of sonosensitiser DVDMS, followed by sonodynamic therapy (SDT) resulted in retarded

Table 1 (*continued*)

Reference	Treatment size	Dose and method of delivery	Animal model Tumour model Implantation site	FUS technology Sonication parameters	Microbubbles	Method to characterize BBB disruption	Findings
							tumour growth and prolonged survival
McDannold 2019 [44]	Carboplatin 371 Da	50 mg/kg IV at the time of FUS	Fischer rats F98 rat glioma caudate putamen	Clinical MRgFUS (ExAblate Neuro, InSightec): 1024-element, 230 kHz hemispherical transducer BL 5 ms, PRF 1.1 Hz, T 55 s AP 119–186 kPa Integrated cavitation monitoring system	Definity, 10 μl/kg	CE-MRI: Gadobutrol (Gadavist), 0.125 mmol/kg	Demonstration of safe, repeatable BBBD with a clinical MRgFUS device in a rat glioma model. Enhanced delivery of carboplatin to the brain was not neurotoxic and significantly reduced tumour growth and prolonged survival
McDannold 2020 [45]	Irinotecan 587 Da	10–20 mg/kg IV	Sprague-Dawley rats F98 rat glioma caudate putanem	Clinical MRgFUS (ExAblate Neuro, InSightec): 1024-element, 230 kHz hemispherical transducer BL 5 ms, PRF 1.1 Hz, T 55 s AP 119–186 kPa Integrated cavitation monitoring system	Definity, 10 μl/kg bolus at start of sonication	CE-MRI: Gadobutrol (Gadavist), 0.125 mmol/kg	BBBD with a clinical MRgFUS device resulted in significantly higher irinotecan concentrations in the brain. While irinotecan delivery to the brain was not neurotoxic, it did not improve outcomes in the F98 glioma model
Wei 2021 [46]	Etoposide 589 Da	5 mg/kg IP immediately after FUS	B6-albino mice MGPP3 mouse glioma striatum	SES FUS transducer (Imasonic): RF 1.5 MH BL 10 ms; PRF 5 Hz; T 120 s AP 0.7 MPa Pulse-echo (imaging) transducer for passive cavitation detection	IHM polydisperse MBs, 0.8E+09 bubbles/ml, 1 μl/g	CE-MRI: Gadodiamide (Omniscan), 0.2 ml IP injection	BBBD with FUS increased intratumoural delivery of etoposide in the brain, resulting in overall survival benefits
Englander 2021 [47]	Etoposide 589 Da	20 mg/kg IP immediately after FUS	B6-albino mice MGPP3 murine glioma brain stem (pons)	SES FUS transducer (Imasonic): RF 1.5 MH BL 10 ms; PRF 5 Hz; T 120 s AP 0.7 MPa Pulse-echo (imaging) transducer for passive cavitation detection	SonoVue or Definity; 100 μl (dose not specified)	(1) CE-MRI: Gadodiamide (Omniscan), 0.2 ml IP; (2) Evans blue	First demonstration of FUS-mediated BBBD in a brainstem tumour (pontine glioma) while preserving normal cardiorespiratory and motor function. FUS increased intra-tumoural etoposide concentration by >5-fold and was safe with repeated (2×) BBB opening
Liposomal formulations (75–120 nm)							
Yang 2012 [55]	Liposomal doxorubicin (DOX) and AP-1-Lipo-DOX (atherosclerotic plaque-specific peptide-1)	Not specified	NOD/SCID mice GBM8401 human glioma striatum	SES FUS transducer (A392S, Panametrics): RF 1.0 MHz. BL 50 ms, PRF 1 Hz, T 60 s, AP 0.7 MPa	SonoVue, 300 μl/kg 10 s before each sonication	micro-SPECT/CT of 111In-labeled AP-1-Lipo-DOX	111In-Lipo-Dox or 111In-AP-1 Lipo-Dox FUS-mediated treatment significantly enhanced accumulation of the drug in the brain tumours

Table 1 (*continued*)

Reference	Treatment size	Dose and method of delivery	Animal model Tumour model Implantation site	FUS technology Sonication parameters	Microbubbles	Method to characterize BBB disruption	Findings
Treat 2012 [33]	Liposomal doxorubicin (DOX)	5.67 mg/kg IV before or after FUS	Sprague-Dawley rats 9L rat glioma left frontal lobe	SES FUS transducer (IHM): RF 1.7 MHz BL 10 ms, PRF 1 Hz, T 60–120 s AP 1.2 MPa	Definity, 10 μl/kg	CE MRI: Gd-DPTA (Magnevist), 0.25 ml/kg IV after FUS	FUS-mediated liposomal DOX treatment significantly reduced 9L rat glioma growth and increased median survival compared to lipo-DOX only
Aryal 2013 [56]	Liposomal doxorubicin (DOX)	5.67 mg/kg IV before each sonication, three weekly treatments	Sprague-Dawley rats 9L rat glioma caudate putamen	SES FUS transducer (IHM): RF 690 kHz BL 10 ms, PRF 1 Hz, T 60 s AP 0.55–0.81 MPa	Definity, 10 μl/kg bolus 9 s before each sonication	CE MRI: Gd-DPTA (Magnevist), 0.25 ml/kg IV after FUS	Multiple FUS sessions enhanced the delivery and therapeutic effect of liposomal DOX in a 9L rat glioma model. Three weekly treatments increased median survival time, however adverse events (brain tissue damage and intratumoural haemorrhage) were observed
Chen 2015 [59]	Folate-conjugated polymersomal doxorubicin (FPD)	5 mg/kg DOX (DOX in FDP: 2 mg/ml) IV	Sprague–Dawley rats C6 rat glioma striatum	SES FUS transducer (A392S, Panametrics): RF 1 MHz BL 50 ms, PRF 1 Hz, T 60s AP 0.7 MPa	IHM des-octanoyl ghrelin-conjugated MB loaded with TGFβ1 inhibitor, 3.4E+ 0.9 MB/ml, size ~1.5 μm; 100 μl/kg IV 3 min before sonication	Extravasation of superparamagnetic iron oxide nanoparticles (SPIONs), (10 mg/kg), T2 weighed MRI imaging	Development of des-octanoyl ghrelin-conjugated MB loaded with TGFβ1 inhibitor (GMBL) to facilitate the binding of MB on the BBB. FUS-mediated delivery of FPD in combination with GMBL enhanced accumulation and antitumour activity of doxorubicin
Aryal 2015 [57]	Liposomal doxorubicin (DOX)	5.67 mg/kg IV before each sonication	Sprague-Dawley rats 9L rat glioma caudate	SES FUS transducer (IHM): RF 690 kHz BL 10 ms, PRF 1 Hz, T 60 s AP 0.55–0.81 MPa	Definity, 10 μl/kg bolus 9 s before each sonication	(1) DCE-MRI: Gd-DPTA (Magnevist), 0.5 ml/kg after FUS; (2) TB, 2.5 ml/kg, after MRI	Characterisation of FUS-induced permeability changes of the blood-tumour barrier in a rat glioma model at different times after tumour implantation using DCE-MRI
Sun 2017 [58]	Liposomal doxorubicin (DOX)	2 mg/kg IV before FUS	Fischer rats F98 rat glioma caudate putamen	Dual-transducer system: two IHM SES FUStransducers (RF 274.3 kHz) mounted at an angle of 102° with respect to each other; Acoustic emission controller	Optison, 200 μl/kg; either as a bolus or as the same bolus followed by a constant infusion (0.08 ml/min)	(1) CE-MRI: Gd-DPTA (Magnevist), 0.25 ml/kg after FUS; (2) Trypan Blue, 0.1 g/kg	Demonstration of successful drug delivery in F98 glioma model by optimizing acoustic parameters of FUS and MB administration
Shen 2017 [60]	Liposomal paclitaxel (PTX-LIPO)	10 mg/kg IV before sonication with MBs	Balb/c nude mice U87 human glioma striatum	SES FUS transducer (IHM): RF 1.1 MHz BL 10 ms, PRF 1 Hz, T 60 s AP 0.64 MPa	IHM lipid MB with perfluoropropane; 0.2 μl/g before sonication	(1) EB; (2) fluorescence dye (IR780) loaded liposomes	FUS BBBD effectively delivered PTX-LIPO for GBM treatment. 2-fold increase in PTX concentration in glioma 3 h after FUS, increased medium survival
Zhao 2018 [61]	shBirc5 loaded liposomes (shBirc5-lipo-NGR)	1 mg of shBic5 per animal	Rats C6 rat glioma right hemisphere	SES FUS transducer (IHM): RF 1 MHz Sonication parameters not	IHM MB loaded with shBirc5-lipo-NGR; 4.0E+07 MB before sonication	EB	Loading of MB-liposome complex with interfering RNA and CD13 targeting (MB-shBirc5-lipo-NGR) with FUS.

Table 1 (*continued*)

Reference	Treatment size	Dose and method of delivery	Animal model Tumour model Implantation site	FUS technology Sonication parameters	Microbubbles	Method to characterize BBB disruption	Findings
				clearly defined, T 3 min AP 1.8 W			Significant therapeutic effect of MB-shBirc5-lipo-NGR on tumour growth and survival time
Papachristodoulou 2019 [62]	LP-O6BTG-C18 – liposome loaded MGMT depleting drug	7.2 mg/kg IV 2 min before FUS; 2 days later: TMZ (10 mg/kg) orally for 5 days	VM/Dk mice SMA-497 mouse glioma right striatum	6-element annular array transducer (Imasonic) BL 10 ms, PRF 1 Hz, T 180 s AP 0.28–0.55 MPa passive cavitation detector	BG8235, 50 µl, 1 µl/s during onication for 50 s	CE-MRI: Gd-DOTA, 50 µl IV; (2) fluorescence dye (DiD) – labeled liposomes, 0.3 µg/kg	FUS-facilitated delivery of the new liposomal MGMT inactivator resulted in significantly prolonged survival of glioma-bearing mice, when combined with temozolomide (TMZ) chemotherapy
Antibody-based treatments (70–100 kDa)							
Kinoshita 2006 [18]	Trastuzumab (Herceptin)	20 mg/kg IV before FUS	Swiss–Webster mice healthy	SES FUS transducer (IHM): RF 690 KHz BL 10 ms, PRF 1 Hz, T 40 s AP 0.6 or 0.8 MPa	Optison, 50 µl	(1) CE MRI: Gd-DPTA (Magnevist), 10 µl IV after FUS; (2) TB, 80 mg/kg	First proof of concept that MRIgFUS technology can be used to deliver a macromolecule locally and noninvasively into the mouse brain through the BBB. The amount of Herceptin delivered to the target tissue correlated with the extent of the BBB opening and was significantly higher in tissues sonicated with 0.8 MPa than 0.6 MPa
Park 2012 [50]	Trastuzumab (Herceptin)	2 mg/kg IV after FUS	Nude rats BT474 human breast carcinoma right frontal lobe	SES FUS transducer (IHM): RF 1.7 MHz BL 10 ms, PRF 1 Hz, T 60 s AP 0.69 MPa	Definity, 10 µl/kg	CE MRI: Gd-DPTA (Magnevist), 0.2 ml/kg IV after FUS	FUS-mediated delivery of Herceptin improved outcomes in breast cancer brain metastases. Significant reduction (up to complete remission) of the tumour volume. Median survival improved by 32%
Chen 2015 [52]	Interleukin-12 (IL-12)	0.3 µg/kg/day IP for 5 days	Sprague–Dawley rats C6 rat glioma right striatum	SES FUS transducer (Sonic Concepts): RF 500 kHz BL 100 ms, PRF 1 Hz, T 90 sAP 0.36–0.7 MPa	SonoVue, 100 µl/kg	EB	FUS-mediated delivery of IL-12 – immunomodulating agent. Significant increase in DOX concentrations in tumours regardless of the stage of tumour growth
Liu 2016 [107]	Bevacizumab (Avastin) 68Ga-labeled	50 mg/kg for 5 weeks followed by FUS	Nude (NU/NU) mice U87 human glioma striatum	SES FUS transducer (Sonic Concepts): RF 400 kHz BL 10 ms, PRF1 Hz, T 60 s, AP 0.35, 0.4, 0.53 MPa	SonoVue, 10 µl/20 g mouse	(1) CE MRI: Gd-DPTA (Magnevist), 0.25 ml/kg IV after FUS; (2) Fluorescent-tagged dextrans (70, 150, and 250 kDa); (3) 68Ga-Bevacizumab PET Imaging	FUS significantly enhanced penetration of Avastin into the brain (5.7- to 56.7-fold) resulting in retarded glioma progression and increase in median survival
Kobus 2016 [51]	Trastuzumab (Herceptin) + Pertuzumab	4 mg/kg – 1st treatment, 2 mg/kg – following	Nude rats MDA-MB-361 human breast	SES FUS transducer (IHM): RF 690 KHz	Optison, 100 µl/kg, bolus before sonication	CE MRI: Gd-DPTA (Magnevist), 0.25 ml/kg IV after FUS	FUS-mediated BBBD in combination with antibody inhibited growth of breast

Table 1 (*continued*)

Reference	Treatment size	Dose and method of delivery	Animal model Tumour model Implantation site	FUS technology Sonication parameters	Microbubbles	Method to characterize BBB disruption	Findings
		weeks, IV before FUS	carcinoma front lobe	BL 10 ms, PRP 1 Hz, T 60 s AP 0.46–0.62 MPa			cancer brain metastasis. However only half of the animals responded to the treatment
Arvanitis 2018 [38]	Ado-trastuzumab-emtansine (T-DM1) antibody–drug conjugate	5 mg/kg IV after FUS	mice BT474 human breast carcinoma	SES FUS transducer (IHM): RF 1.025 MHz. BL 10 ms, PRF 1 Hz, T 120 min AP 0.48 MPa	Definity, 20 µl/kg during sonication	Immunohistochemistry	FUS-mediated increase of early extravasation (2-fold) and penetration (4 ± 7 vs. 12 ± 4 µm) of T-DM1
Brighi 2020 [53]	EphA2-4B3 antibody, 89Zr-radiolabelled	~4 MBq of ^{89}Zr-radiolabelled EphA2-4B3	NOD/SCID mice WK1 human glioma striatum	LP-100 FUS system (FUS Instruments) SES FUS transducer: RF 1.1 MHz BL 10 ms, T 120 s AP 0.85 MPa	Definity, 200 µl of 2% dilution (~160 µl/kg)	(1) CE-MRI: Gadobutrol (Gadovist), 0.1 mmol/kg; (2) PET-CT for quantifying antibody uptake (1 day after FUS)	FUS locally increased antibody uptake in the targeted regions of the tumour, while leaving untargeted regions unaffected
Sheybani 2021 [54]	CD47 antibody, 89Zr-radiolabelled	8 or 32 mg/kg 15 min before FUS	C57BL/6 mice GL261 mouse glioma striatum	RK-100 FUS system (FUS Instruments) SES FUS transducer: RF 1.14 MHz 0.5% duty cycle, T 120 min AP 0.4 MPa	IHM albumin-shelled MB, 1.0E+05 MB/g bolus before sonication	(1) CE-MRI: MultiHance (gadolinium-based contrast agent) 0.05 ml of 105.8 mg/ml; (2) ImmunoPet [89Zr]-mCD47	Demonstration that timing of Ab injection relative to FUS-mediated BBBD is critical. Post-FUS injection increased Ab delivery to gliomas. Repeated sessions of FUS extended survival in glioma-bearing mice
Ye 2021 [73]	anti-programmed cell death-ligand 1 antibody (aPD-L1)	24 µl of 2.4 mg/ml; Intranasal, 0.5 h before FUS	Swiss–Webster mice GL261 mouse glioma brain stem	VIFU 2000 (Alpinion) system SES FUS transducer: RF 1.5 MHz BL 6.7 ms, PRF 5 Hz, T 60 s AP 0.43 MPa	IHM MB (4–5 µm) 30 µL of 8.0E+08 MBs/ml bolus before sonication	Ex vivo near-infrared fluorescence 800CW-aPD-L1	Proof of principle of FUS-mediated intranasal brain drug delivery (FUSIN): enhanced accumulation of aPD-L1 at the FUS-targeted brainstem
Nanoparticle-based treatments (7–300 nm)							
Chen 2010 [108]	BCNU on magnetic nanoparticles (MNP) ~10–20 nm	0.5, 1, 5 mg/kg	Sprague-Dawley rats C6 rat glioma site not specified	SES FUS transducer (Imasonics): RF 400 kHz BL 10 ms, PRF 1 Hz, T 30 s AP 0.62 MPa	SonoVue, dose not specified	CE-MRI: Gd-DPTA (Magnevist), 0.1 mmol/kg IV before MRI	Combination of FUS with magnetic targeting (MT) enhanced localization of BCNU-MNP to gliomas without damaging healthy regions
Liu 2010 [109]	Epirubicin on magnetic nanoparticles (MNP) ~12 nm	Not specified	Sprague-Dawley rats C6 rat glioma striatum	SES FUS transducer (Imasonics): RF 400 kHz BL 10 ms, PRF 1 Hz, T 120 s AP 0.62 MPa	SonoVue, 100 µl/kg	(1) CE MRI: Gd-DPTA (Magnevist), 0.1 mmol/kg IV before MRI; (2) EB, after sonication	Combined use of FUS and MT of Epirubicin-MNP. The combination of FUS and 6 h of MT increased epirubicin compared with FUS alone
Fan 2013 [67]	DOX loaded superparamagnetic iron oxide nanoparticles (SPIO) conjugated lipid MB (DOX-SPIO-MB)	DOX 472.5 µg, SPIO dose of 337.5 µg per animal	Sprague-Dawley rats C6 rat glioma site not specified	SES FUS transducer (Imasonics): RF 400 kHz PRF 1 Hz, T 90 s AP 325 kPa	IHM DOX loaded SPIO-conjugated MBs, mean size 1 µm, ~1.5E+10 MB per animal	(1) EB, 100 mg/kg IV 5 min before sonication; (2) Dynamic susceptibility contrast MRI (DSC-MRI) for SPIO nanoparticles	Multifunctional MB conjugated with SPIO nanoparticles loaded with DOX significantly enhanced local SPIO deposition in tumour regions by 22.4%
Diaz 2014 [63]	Gold nanoparticles (GNP) PEG-coated 50 nm	17 mg/kg HAuCl4 IV 8 min before FUS	Wistar rats 9L rat glioma frontal lobe	SES FUS transducer (IHM): RF 551.5 kHz BL 10 ms, PRF 1 Hz, T 120 s	Definity, 20 µl/kg	DCE-MRI: gadodiamide (Omniscan), 0.2 ml/kg	Demonstration of FUS-mediated delivery of GNP to the tumour margins with the potential to be used as optical

Table 1 (*continued*)

Reference	Treatment size	Dose and method of delivery	Animal model Tumour model Implantation site	FUS technology Sonication parameters	Microbubbles	Method to characterize BBB disruption	Findings
				AP ~ 0.23 MPa Real-time monitoring of MB emissions (hydrophone)			tracking agents and for the delivery of therapeutic agents
Fan 2016 [80]	DOX conjugated to SPIO nanoparticles ~50 nm	4 mg of SPIO-DOX loaded MBs IV before FUS	Sprague-Dawley rats C6 rat glioma site not specified	SES FUS transducer (V302, Panametrics): RF 1 MHz PRF 1 Hz, T 4 min AP 0.3 MPa	IHM lipid MB loaded with SPIO-DOX complexes	(1) T2* MRI for SPIO nanoparticles; (2) EB, 100 mg/kg	Fabrication and optimisation of SPIO-DOX complexes loaded onto MBs. FUS combined with MT enhanced targeted deposition of DOX (25.7-fold increase)
Timbie 2017 [65]	Cisplatin loaded polimeric brain penetrating nanoparticles ~60 nm	2.5 mg/kg IV with MBs before FUS	Fisher rats 9L and F98 rat gliomas striatum	SES FUS transducer (FUS Instruments): RF 1.14 MHz 0.5% duty cycle, T 120 min AP 0.6 and 0.8 MPa	IHM albumin-shelled MB, 1.0E+05 MB bolus before each sonication	(1) CE-MRI: Gd-DPTA (Magnevist), 0.25 µl/g IV after sonication; (2) 60 nm fluorescently labeled BPNs, 15 µg/g IV before sonication	FUS-mediated delivery of 60 nm cisplatin-nanoparticles resulting in improved animal survival
Coluccia 2018 [64]	Cisplatin conjugated gold nanoparticles ~7 nm	0.5 mg/kg IV after MBs at the time of FUS	NSG mice U251 human glioma frontal lobe	SES FUS transducer (INM): RF 1.68 MHz BL 10 ms, PRF 1 Hz, T 120 s Acoustic emission controller to modulate AP	Definity, 20 µl/kg bolus at start of sonication	CE-MRI: Gadobutrol (Gadovist), 0.1 ml/kg; IV after MBs and GNP-UP-Cis before FUS	FUS-mediated delivery of Cisplatin conjugated gold nanoparticles greatly reduced the growth of U251 GBM tumours
Fan 2019 [66]	Boron-containing polyanion nanoparticles coupled with cationic MBs	0.035 mg/kg	C57BL/6 mice GL261 mouse glioma striatum	SES FUS transducer (V302, Panametrics): RF 1 MHz PRF 1 Hz, T 60 s AP 0.5 MPa	IHM cationic MB coated with PEG-b-PMBSH, 50 µl, retro-orbital injection	(1) EB, 100 mg/kg; (2) LA-ICP-MS of boron distribution	Successful FUS-mediated delivery of polyanionic boron (PEG-b-PMBSH) bound to cationic MB. Increased boron uptake in tumours immediately after FUS with 3-fold increase in tumour-to-normal brain ratio
DNA, virus, cell-based treatments							
Alkins 2013 [69]	Human NK-92 cells loaded with superparamagnetic iron oxide nanoparticles	1.0E+09 cells/sqm of body surface area IV at the time of sonication	Nude rats MDA-MB-231 human breast carcinoma frontal striatum	SES FUS transducer (IHM): RF 551.5 kHz BL 10 ms, PRF 1 Hz, T 120 s AP 0.32–0.35 MPa Acoustic emission controller to modulate AP	Definity, 20 µl/kg	CE MRI: Gadodiamide (Omniscan), 0.2 ml/kg	First proof-of-concept of FUS-mediated targeting of immune cell therapies to brain tumours. 5-fold increase of NK-92 to tumour cells ratio (1:100) when NK cells were present in the vasculature at the time of sonication
Fan 2016 [68]	pFLuc plasmid DNA -loaded cationic MBs	Not specified	Sprague-Dawley rats C6 rat glioma left hemisphere	SES FUS transducer (V302, Panametrics): RF 1 MHz PRF 5 Hz, T 60 s, AP 0.7 MPa	IHM folate-conjugated DNA-loaded cationic MBs, ~4.3 µm of 4.0E+0.7 MB/ml	(1) EB, 100 mg/kg, 10 min before FUS; (2) bioluminescence imaging	Development of multifunctional MB for FUS-mediated gene delivery/ therapy. Better gene transfection efficiency with folate conjugated MB
Noroozian 2019 [77]	Recombinant adeno-associated virus (rAAV)	3.0E+09 vg/g IV	mice or rats healthy	RK-300 FUS system (FUS Instruments) SES FUS transducers: Rats: RF 551.5 kHz	Definity, 20 µl/kg	CE-MRI: Gadobutrol (Gadovist), 0.1 ml/kg	The dose of IV injected rAAV variants that can cross the BBB can be reduced by 100 times when facilitated by FUS-

Table 2
Preclinical studies investigating FUS-mediated sterile inflammatory response.

Reference	Animal model	FUS technology Sonication parameters	Microbubbles	Treatment area	Readouts	Findings
Kovacs 2017 [117]	Sprague-Dawley rats	RK-100 FUS system (FUS Instruments) SES FUS transducer: RF 590 KHz BL 10 ms; PRP 1 Hz; T 120 min AP 0.4 MPa	Optison, 500 µl/kg	Frontal cortex anterior to the lateral ventricle	0.5, 1, 2, 6, 12, 24 h and 6 days post-FUS: (1) Rat Bio-Plex Cytokine 24-Plex group I assay (2) ELISA (SDF1, BDNF, MMP9, FGF, ICAM, HSP70, HGF) (3) qPCR (RT2 Profiler PCR Array Rat NFκB Signalling Pathway) (4) Western blot (Akt, GSK3b, ERK, JNK, p38-MAPK) (5) IHC (ICAM, GFAP, Iba1, albumin, CD68)	FUS-induced a cascade of molecular and cellular changes consistent with the induction of a SIR: – Induction of HSP70 and proinflammatory cytokines (TNFα, IL1α, IL1β, IL18, and IFNγ); – Transcriptomic changes associated with NFκB pathway; – Upregulation of ICAM, activated astrocytes and microglia up to 24 post-sonication; – (4) Tropism of systemic CD68+ macrophages (several days post-sonication)
McMahon & Hynynen 2017 [83]	Sprague-Dawley rats	RK-100 FUS system (FUS Instruments) SES FUS transducer: RF 551.5 KHz BL 10 ms; PRP 1 Hz; T 120 min AP 0.290 MPa or acoustic emission controller, starting AP 0.128 MPa	Definity, 10 µl/kg and 100 µl/kg	Three sonication locations per animal, each with a different sonication scheme	6 h and 4 days post-FUS: (1) qPCR (RT2 Profiler PCR Array Rat NFκB Signalling Pathway) (2) T2W-MRI (oedema and haemorrhage) (3) histology (red blood cells, leucocytes, microglia)	High MB dose resulted in upregulation of genes associated with acute inflammation, immune response, and apoptosis. The effect was accompanied by oedema, neuronal degeneration, leukocyte infiltration, and microhemorrhage. These effects were not significant at low MB dose
McMahon 2017 [118]	Sprague-Dawley rats	RK-100 FUS system (FUS Instruments) SES FUS transducer: RF 551.5 KHz, BL 10 ms; PRP 1 Hz; T 120 min Acoustic emission controller, starting AP 0.128 MPa	Definity, 20 µl/kg	Dorsal hippocampus	6 h and 24 h post-FUS: transcriptional changes in hippocampal microvessels (Affymetrix Rat 2.0 ST array)	FUS-induced transient increase in transcription of inflammatory-related genes in microvessels (e.g. Sele, Cxcl1, Ccl3, and Ccl2) largely returning to baseline by 24 h. Some inflammatory markers (e.g. C3, Ccl6, Gfap, and Itgb2) remained significantly upregulated at 24 h
McMahon 2018 [120]	Sprague-Dawley rats	LP-100 FUS system (FUS Instruments) SES FUS transducer: RF 551.5 KHz BL 10 ms, PRP 1 Hz; T 120 min Acoustic emission controller, starting AP 0.128 MPa	Definity, 20 µl/kg	Dorsal hippocampus	7, 14, and 21 d post FUS: (1) IHC (GLUT-1, VEGFA) (2) blood vessel density (3) newborn endothelial cell density	FUS-mediated angiogenic response in rat hippocampus. Blood vessel density and newborn endothelial cell density modestly elevated at 7 and 14 d post-FUS, returning to baseline at 21 d
Sinharay 2019 [121]	Sprague-Dawley rats	RK-100 or LP-100 FUS system (FUS Instruments) SES FUS transducer: RF 548 KHz BL 10 ms; PRP 1 Hz; T 120 min Acoustic emission controller, starting AP 0.144 MPa	Optison, range 584–361 µl/kg at a rate of 1.66 µl/s	Frontal cortex and right hippocampal regions. Single and multiple FUS sessions	After single and multiple sonications: 1) PET [18F]DPA-714 – tracer translocator protein (TSPO) – a biomarker of neuroinflammation; (2) IHC (GFAP, Iba1)	Increased binding of [18F]DPA-714 in sonicated areas, less in hippocampus compared to frontal cortex. No cumulative increase of SIR after multiple sonications (2 and 6 separated by 7 days)
Brighi 2020 [53]	NOD/SCID mice	LP-100 FUS system (FUS Instruments) SES FUS transducer: RF 1.1 MHz BL 10 ms; T 120 s AP 0.85 MPa	Definity, 200 µl of 2% dilution (~160 µl/kg)	Tumour implanted in striatum (100–300 mm^3)	IHC (GFAP and Iba1)	Substantial astrogliosis and microgliosis in FUS-treated tumour regions 3 days post-FUS
Pascal 2020 [96]	CD1 mice	6-element annular array transducer (Imasonic) RF 650 kHz BL 10 ms; PRF 1 Hz; T 120 s Acoustic pressures: 0.15 MPa, 0.25 MPa, 0.35 MPa, 0.45 Mpa. Passive cavitation detector for acoustic emissions	Definity, 10 µl/kg and 250 µl/kg	Left hemisphere	(1) Histopathology (H&E) for haemorrhage and oedema (2) IHC (Iba1, TMEM119, GFAP)	Mild histologic changes and activation of the acute SIR at low APs independent of MB dose. Higher APs (0.25 MPa or above) resulted in more severe haemorrhage, oedema and SIR response especially with the higher MB dose
McMahon 2020 [93]	Sprague-Dawley rats	RK-100 FUS system (FUS Instruments) SES FUS transducer: RF 580	Definity, 20 µl/kg	Dorsal hippocampus	(1) Rat Cytokine array (Q2, Raybiotech)	Increased expression of key inflammatory markers (ICAM1, MCP1, GFAP) in sonicated areas 2

Reference	Animal model	FUS technology Sonication parameters	Microbubbles	Treatment area	Readouts	Findings
		KHz BL 10 ms, PRP 1 Hz; T 120 min Acoustic emission controller, starting AP 0.128 kPa			(2) ELISA (GFAP) (3) IHC (GFAP)	days post-FUS. Indications of astrocyte activation 10 days post FUS. DEX expedited the restoration of BBB integrity and abrogated the SIR-related changes
Poon 2021 [123]	Transgenic EGFP Wistar rats	Cylindrical FUS transducer (IHM) RF 1 MHz BL 10 ms; PRF 1 Hz; T 120 min AP 0.28–0.55 MPa	Definity, 40 μl/kg	Hemisphere (with cranial window created in the parietal bone)	(1) Two-photon fluorescence microscopy (2PFM) with fluorescent dextrans (2) IHC (RECA1, CD31, GLUT1 (blood vessels); GFAP (astrocytes); MPO (neutrophils)	FUS-induced intravascular leukocyte activity indicative of acute inflammation. Neutrophils identified to be a key participating leukocyte. The cellular response takes place immediately after the onset of FUS
Chen 2021 [7]	Fischer rats C6 glioma	SES FUS transducer (Imasonics) RF 400 kHz BL 10 ms; PRF 1 Hz; T 120 s AP 0.63 or 0.81 MPa	SonoVue, dose not specified (? 100 μl/kg)	Tumour	5 h and 7 d post FUS: IHC: CD4, CD8 (T lymphocytes); FOXP3 (T-regs); CD68 (Macrophages)	A significant increase in CD4+ and CD8+ lymphocytes 7 days after 0.81 MPa FUS treatment with no significant changes of macrophage or T-reg lymphocyte counts. No statistically changes detected after treatment with lower FUS exposure level